5 RESULTS

5.1 Role of STAT3 in transformation

While the oncogenic capacity of activated STAT3 has been demonstrated in rodent cells (Bromberg *et al.* 1999), its transforming potential in humans is less established. STAT3 is constitutively activated in approximately 80% of primary breast tumors, unlike in normal breast epithelial cells (Garcia *et al.* 2001). Therefore, MCF10A cells, spontaneously immortalized, non-transformed human breast epithelial cells (Soule *et al.* 1990), were selected to study the effects of constitutive STAT3 activation.

5.1.1 Role of STAT3 activation in human cells

5.1.1.1 No constitutive STAT3 phosphorylation in MCF10A cells

MCF10A cells do not present constitutive phosphorylation of STAT3 (Garcia *et al.* 1997), and their cultivation requires addition of EGF to the growth medium (Soule *et al.* 1990). In order to investigate the effect of the presence of EGF and serum on the activation status of STAT3, its phosphorylation was studied in this cell line in full medium[1], and in starvation medium[2]. As controls, MDA-MB-468 cells, a breast tumor cell line, and DU145, prostate tumor cells, both with constitutively activated STAT3 were used (Garcia *et al.* 1997;Lou *et al.* 2000).

[1] i.e. D-MEM/Ham12 supplemented with 10% horse serum, 20 ng/ml EGF, 2 mM L-Glutamine, 100 ng/ml Choleratoxin, and 500 ng/ml Hydrocortison

[2] i.e. D-MEM/Ham12 supplemented with 2 mM L-Glutamine, 100 ng/ml Choleratoxin, and 500 ng/ml Hydrocortison

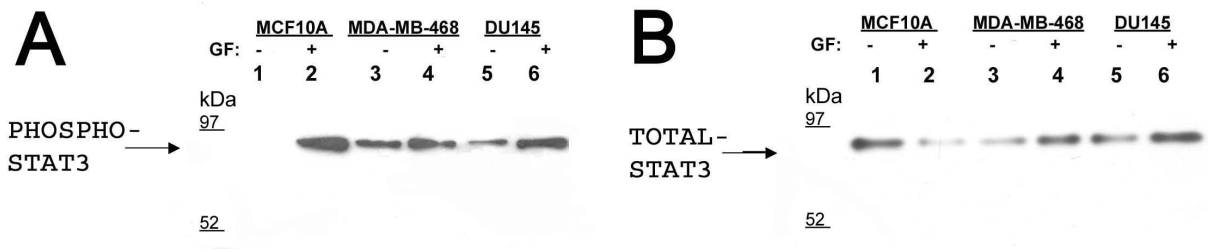

Fig.6. STAT3 is not constitutively phosphorylated in MCF10A cells. Cells were plated on 6-well plates, and the phosphorylation of STAT3 was analyzed in MCF10A, MDA-MB-468, and DU145 cells, in the presence of full culture medium (+), or upon overnight starvation (-). Whole cell lysates were prepared and run on SDS-PAGE (10% polyacrylamide), and analyzed by Western blotting using a phospho-STAT3 specific (A), or a STAT3 (B) antibody.

It was found that MCF10A cells require exogenous growth factor stimulation for STAT3 phosphorylation (Fig.6), whereas DU145 and MDA-MB-468 show activation of this STAT in the absence of these additives. Other non-transformed cells, such as NIH3T3 cells, behave similarly to MCF10A cells, and also require the addition of growth factors for phosphorylation of STAT3 (unpublished data).

5.1.1.2 Proliferation of MCF10A cells is growth factor dependent

Transformed cells present several atypical characteristics, such as growth factor independence for proliferation, apoptosis resistance, anchorage independence and the capacity to form tumors in nude mice (Franks and Teich 1997;Alberts *et al.* 2002;Lodish *et al.* 2003). In order to test the phenotype of MCF10A cells, the impact of growth factors on proliferation and apoptosis was analyzed in MCF10A cells.
Inhibition of STAT3 has been found to suppress the growth of breast cancer cells *in vitro* (Burke *et al.* 2001). Since MCF10A cells showed phosphorylated STAT3 in full medium, but not upon starvation (Fig.6), their proliferation and apoptosis rates were measured in the presence and absence of activated STAT3 (i.e. in full medium, and upon overnight starvation, respectively). It turned out that STAT3 is phospohorylated when these cells proliferate, but is inactive otherwise. Furthermore, MCF10A cells go into apoptosis in the absence of STAT3 stimulation. Therefore, this cell-line is growth factor dependent and not transformed, as opposed to DU145, which survive even in the absence of serum and growth factors.

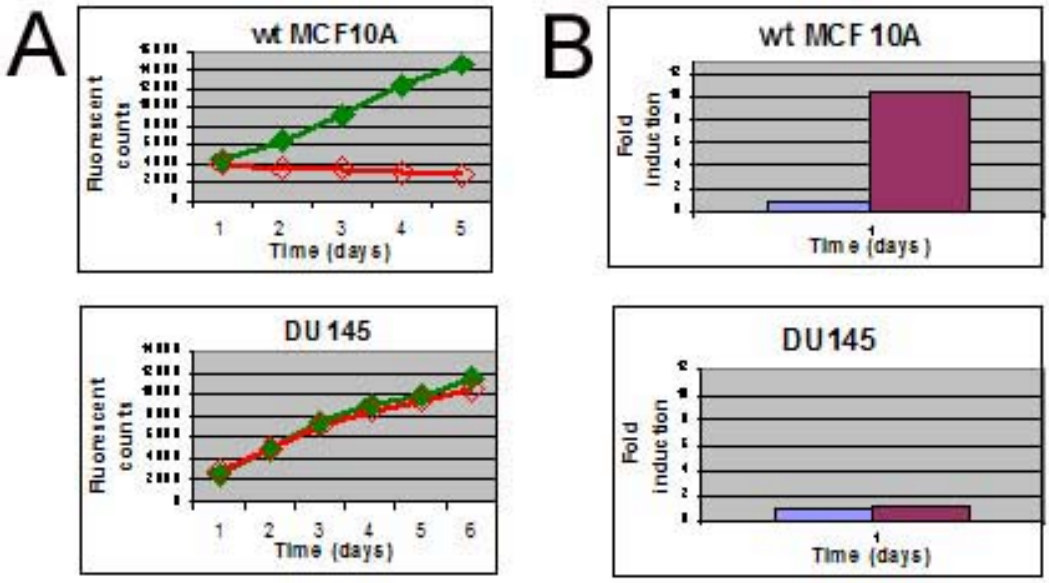

Fig.7. MCF10A cells are growth factor dependent: they proliferate in the presence of growth factors and undergo apoptosis in their absence. A) 3000 cells/well were seeded on a 96-well plate, and, when attached, either kept in full medium or starved overnight. At the indicated time points, cell numbers were deduced by the measurement of mitochondrial activity using the AlamarBlue assay. Green shows proliferation under full medium, red under starvation conditions. B) 2000 cells/well were seeded on a 384-well plate and, several hours later, either left untreated or starved. 48 h later, apoptosis was measured by the caspase-3 activation assay. The fold induction was calculated setting as reference the values in full medium of each respective cell line. Shown are the mean values and standard deviations of four measurements. Blue (resp violet) apoptosis in full medium (resp upon starvation).

5.1.1.3 Growth of MCF10A cells is anchorage dependent

A second parameter of the transformation status of tumor cells is the ability to grow when their anchorage is limited, e.g. in soft agar medium. To confirm that wt MCF10A cells are not transformed, their anchorage dependence was evaluated by their capacity to form colonies in soft agar. NIH-v-Src-TKS3, which are NIH3T3 cells stably transfected with v-Src and the STAT3 reporter pLucTKS3 (Turkson *et al.* 1999), were used as positive control. These cells are transformed and grow in soft agar (Campbell *et al.* 1997;Campbell *et al.* 2001;Johnson *et al.* 1985).

MCF10A cells did not form colonies, as opposed to NIH3T3-TKS3 (Fig.8). Both the growth factor dependence (Fig.7) and the anchorage dependence observed in the colony formation assay indicated that MCF10A cells are non-transformed cells.

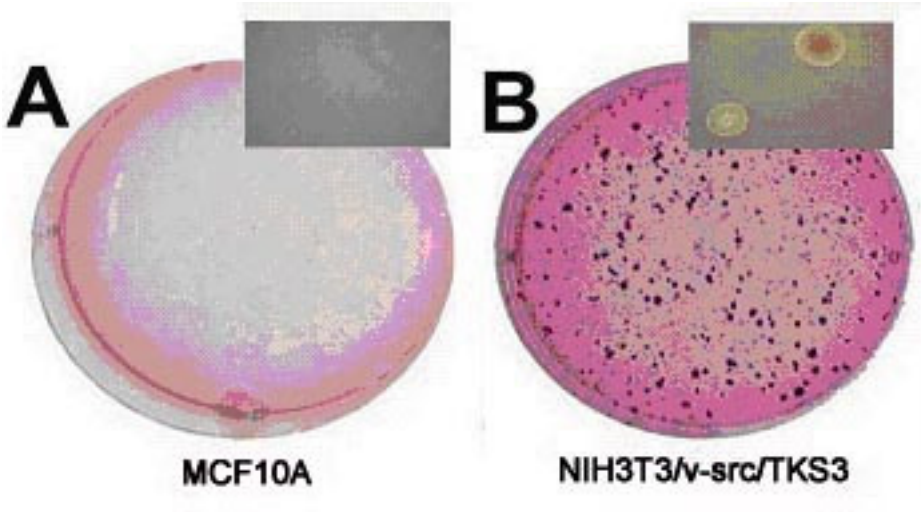

Fig.8. MCF10A cells are non-transformed: they do not form colonies in soft agar. 6000 cells were seeded on a 6-well plate in 0.5% agar, over a 1% agar underlayer. Every 3 to 4 days, fresh medium was added, and after 14 days, colonies were stained with iodonitrotetrazoliumchlorid. A) MCF10A wt cells B) NIH-v-Src-TKS3 cells. Insert shows a 200-fold magnification.

5.1.1.4 Constitutive phosphorylation of STAT3 in MCF10A cells stably transfected with v-Src

Src, a tyrosine kinase originally identified in the genome of the Rous Sarcoma virus, is a potent oncogene, activated in many cancers. There is a strong correlation between Src activation and breast cancer (Lee *et al.* 1999), and its activity has also been directly correlated with the progression of this disease (Summy and Gallick 2003).

Src can directly phosphorylate STAT3 (Cao *et al.* 1996), and STAT3 activation has been found to be essential for the transforming capacity of v-Src (Bromberg *et al.* 1998). Therefore, a constitutively active form of Src ($pp60^{v\text{-}Src}$) (Kmiecik and Shalloway 1987) was used to induce STAT3 phosphorylation, with the aim of transforming MCF10A cells.

MCF10A cells were transfected with pM/v-Src and pEF/pGK/puroPA vectors. After selection with 1 µg/ml puromycin, the resistant cells were cloned. Several clones presenting incorporation of v-Src were identified (Fig.9A). Clone MCF10A-v-Src-B3, showing stable expression of v-Src and strong constitutive phosphorylation of STAT3 (Fig.9B) was used for the following assays.

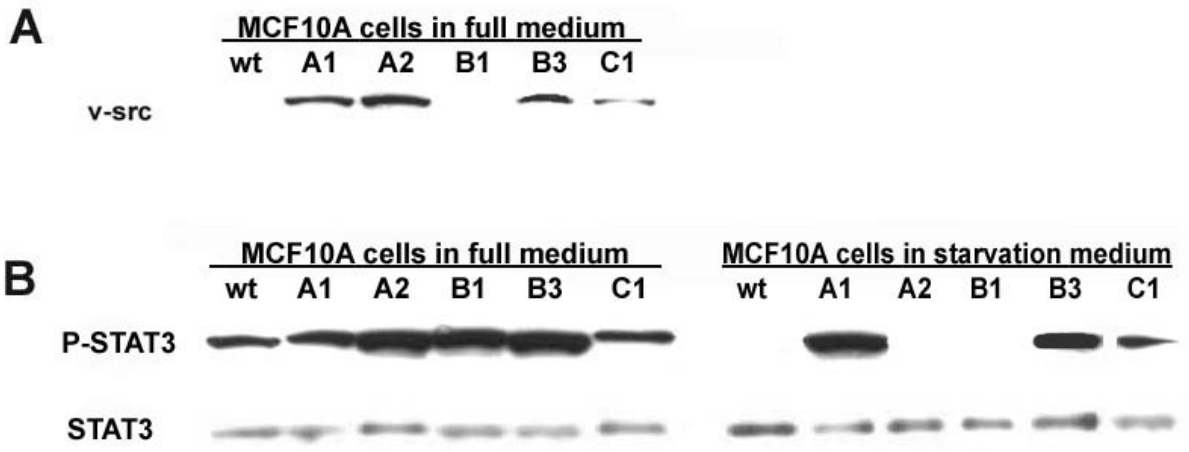

Fig.9. STAT3 is constitutively phosphorylated in MCF10A-v-Src-B3. Whole cell lysates of confluent 6-well plates were prepared and run on SDS-PAGE (10% polyacrylamide), and analyzed by Western blotting. A) The expression of v-Src in the stably transfected MCF10A-v-Src clones was tested with a v-Src antibody. B) The phosphorylation of STAT3 in full culture medium (+), or upon overnight starvation (-) was analyzed using a phospho-STAT3 specific, and a STAT3 antibody.

5.1.1.5 The proliferation of MCF10A-v-Src cells is growth factor independent

The consequences of constitutive STAT3 phosphorylation in v-Src expressing MCF10A cells were analysed under starvation conditions, and compared to wt-MCF10A cells. As expected, both cell lines proliferated at a similar rate in the presence of full medium, but only MCF10A-v-Src-B3 cells kept on multiplying under starvation conditions (Fig.10A). Accordingly, MCF10A-v-Src-B3 cells did not show caspase activation upon starvation, while wt-MCF10A did (Fig.10B).

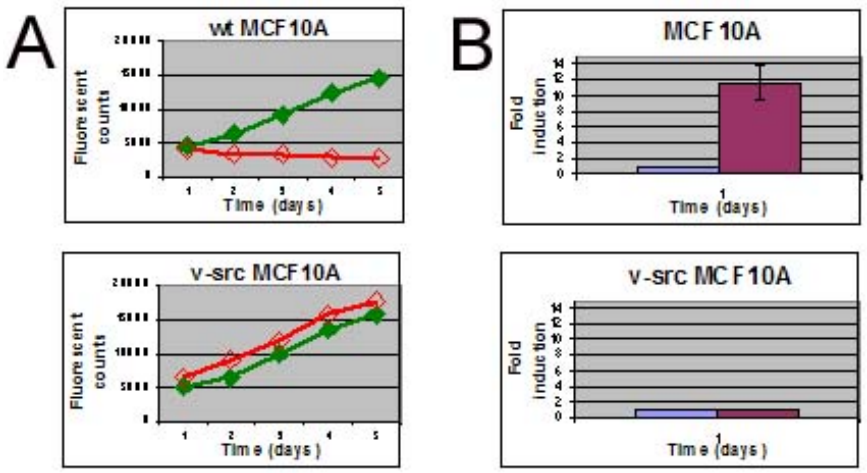

Fig.10. MCF10A-v-Src-B3 cells proliferate and do not undergo apoptosis in the absence of EGF and serum. A) 3000 cells/well of either MCF10A or MCF10A-v-Src-B3 were plated on a 96-well plate, and, when attached, either kept in full medium or starved overnight. At the indicated time points, cell numbers were deduced by the measurement of mitochondrial activity using the AlamarBlue assay. Green shows proliferation under full medium, red under starved conditions. B) MCF10A or MCF10A-v-Src-B3 were seeded on a 384-well plate, and, when attached, either left untreated or starved. 72 h later, apoptosis was measured by determination of caspase-3 activity. The fold induction was

calculated setting as reference the values in full medium of each respective cell line. Shown are the mean values and standard deviations of four measurements. Blue (resp violet) apoptosis in full medium (resp upon starvation).

5.1.1.6 MCF10A-v-Src-B3 cells form colonies in soft agar

The anchorage dependence of MCF10A-v-Src-B3 cells was tested in the colony formation assay in soft agar. It was found that these cells formed colonies. MCF10A cells were used as negative, and NIH-v-Src-TKS3 cells as positive control. MCF10A-v-Src-B3 cells showed a certain anchorage independence, but fewer and smaller colonies were obtained with MCF10A-v-Src-B3 cells compared to those obtained with NIH-v-Src-TKS3 cells. This indicates that the transformation status of NIH-v-Src-TKS3 cells might be more advanced than that of MCF10A-v-Src-B3 cells.

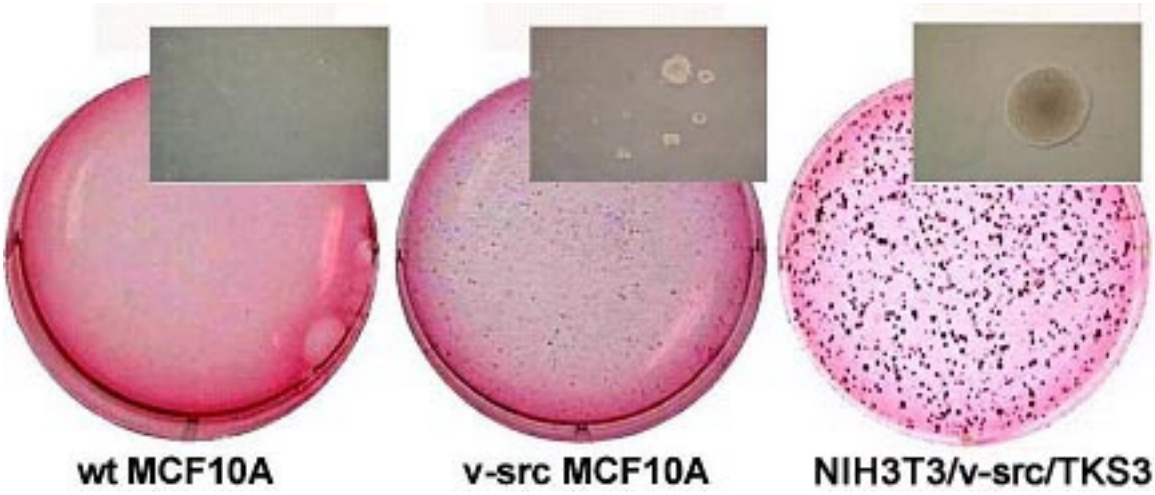

Fig.11. MCF10A-v-Src-B3 cells form colonies in soft agar. 6000 cells of the indicated cell lines were seeded on a 6-well plate in 0.5% agar, over a 1% agar underlayer. 14 days later, colonies were stained with iodonitrotetrazoliumchlorid. Insert shows a 200-fold magnification

In summary, stable expression of v-Src in MCF10A induced changes in this cell line, probably several, one of which was the constitutive phosphorylation of STAT3. Phenotypically, MCF10A-v-Src-B3 cells acquired some typical properties of transformed cells, such as growth factor independent proliferation, resistance to apoptotic stimuli, and anchorage independence.

5.1.1.7 MCF10A stably transfected with v-Src do not generate tumors in immunosuppressed mice

Another property of transformed cells is their capacity to form tumors in immunosuppressed mice (Stanbridge and Perkins 1976). This was evaluated next, and it turned out that neither MCF10A, nor MCF10A-v-Src-B3, nor NIH3T3 cells produced tumors. However, large tumors (over 600 cm^3) grew in all mice injected with NIH-v-Src-TKS3.

Therefore, even though showing increased proliferation, survival and anchorage independence, as compared to wt-MCF10A cells, MCF10A-v-Src-B3 could not be considered as completely transformed.

Altogether, these results might indicate that MCF10A cells require additional mutations to reach full transformation, and that the sole activation of STAT3 might not be oncogenic in this human cell-line.

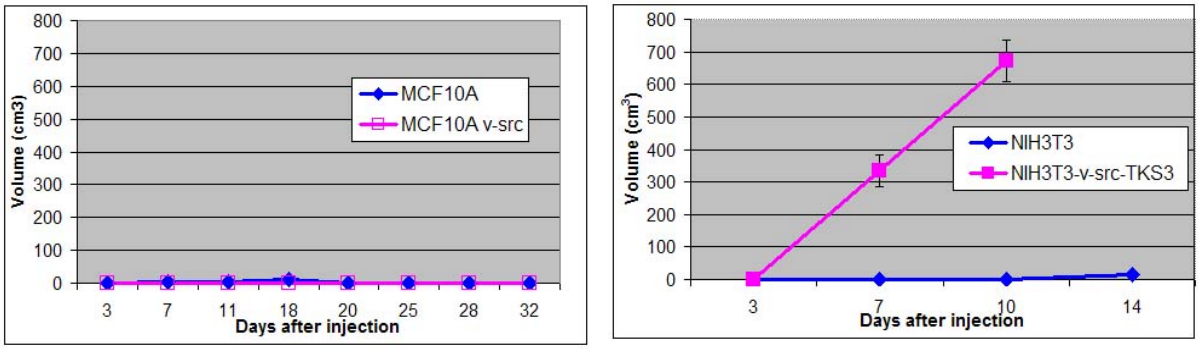

Fig.12. NIH3T3-TKS3 produce tumors in immunosuppressed mice, but MCF10A v-Src do not. $5x10^6$ cells/100 µl PBS of the indicated cells were injected subcutaneously into the back of female, inbred SCID mice (n=6 per group). One of the mice injected with NIH3T3-TKS3 had to be sacrificed at day 7 due to its extreme tumor growth on the leg, and all other mice injected with this cell line at day 10.

5.1.2 Consequences of STAT3 down-regulation in transformed human cells

STAT3 exists in two splicing variants, STAT3α being the active isoform. However, cells can also produce another splice variant, STAT3β, which has a replacement of residues 716 to 770 by a sequence of seven amino acids, FIDAVWK. The

physiological role of STAT3β is not yet fully understood, but experimentally it is commonly used as a DN tool to inhibit STAT3α (Niu *et al.* 1999;Niu *et al.* 2001).
The STAT3 crystal structure was obtained with residues 127 to 722 of STAT3β, i.e. with a N-terminal truncation (Becker *et al.* 1998). As can be appreciated in the solved structure, STAT3β binds the DNA. However, it does not recruit other factors required for the initiation of transcription (Caldenhoven *et al.* 1996). This is why this family member is able to inhibit the activity of STAT3α (Niu *et al.* 1999;Niu *et al.* 2001).
Since constitutive STAT3 activation of DU145 cells has been described (Lou *et al.* 2000), and this cell line shows STAT3 phosphorylation under starvation conditions (Fig.6B), these cells were chosen to test the consequences of STAT3 inhibition. Furthermore, they can produce tumors in nude mice (Church *et al.* 1999), and are therefore appropriate for testing the effects of STAT3 inhibition *in vivo*.

5.1.2.1 Induction of DN-STAT3 using the ecdysone system

DN-STAT3 was amplified from the pSG5 human-STAT3β vector (Fig.13A). The product was then cloned into the pIND/V5-His-TOPO plasmid. Out of nineteen tested clones, eleven (clones 1, 2, 3 5, 6, 7, 12, 13, 14, 17, and 19) incorporated STAT3β in the right orientation (Fig.13B). The results of clones 1, 3 and 19 were confirmed by sequencing.

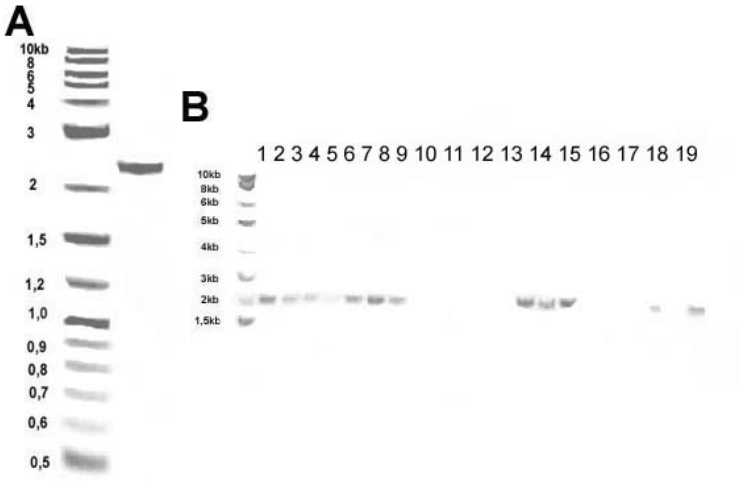

Fig.13. Subcloning of human STAT3β into pIND/V5-His-TOPO vector. A) STAT3β was amplified from pSG5 human-STAT3β vector by PCR with the 5'ATGGCCCAATGGAATCAGCT3' and 5'AATTCACATGGGGGAGGTAG3' primers. The PCR product was analyzed by DNA electrophoresis, and showed the size of human STAT3β. B) Human STAT3β was cloned into pIND/V5-His-TOPO vector, and nineteen clones were screened by PCR for incorporation of DN-STAT3 in the right orientation, using 5'ATGGCCCAATGGAATCAGCTAC3' and 5'TAGAAGGCACAGTCGAGG3' as primers. Eleven clones showed incorporation of STAT3β in the right orientation.

5.1.2.1.1 Ponasterone induction of DN-STAT3 in stably transfected DU145 cells does not trigger changes in the phenotype of these cells

DU145 were stably transfected with pVgRXR and pIND/hSTAT3β. After four weeks of selection with 500 µg/ml zeocin and 100 µg/ml hygromicin, clones were picked and expanded for three additional weeks. In order to check for STAT3β induction capacity, cells were treated with 5 µM ponasterone, and compared with wt DU145 cells. It was found that nine clones expressed STAT3β upon stimulation, although at much lower levels than endogenous STAT3α. Furthermore, five of the positive clones expressed STAT3β even in the absence of ponasterone.

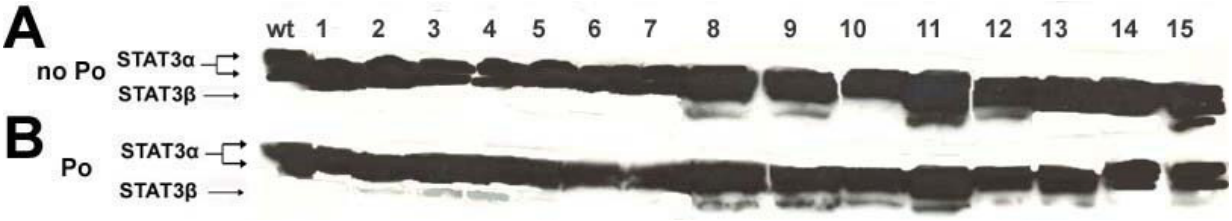

Fig.14. Screening for STAT3β expression in DU145 cells stably transfected with pIND/hSTAT3β. DU145 cells were transfected with pVgRXR and pIND/hSTAT3β. Hygromicin and zeocin resistant cells were cloned. After expansion of the clones, wt DU145 and fifteen clones were plated in 6-well plates and either treated with ponasterone or left untreated. Wt DU145 cells were used as control. Cells were harvested 24 h after treatment, and whole cell lysates were prepared, run on SDS-PAGE (4 to 12% polyacrylamide) and analyzed by STAT3 Western blotting. A) Untreated cells B) cells treated during 48 h with 5 µM ponasterone.

All the clones expressing STAT3β were checked for a phenotype in proliferation and apoptosis. However, upon treatment with ponasterone no significant change was observed in proliferation, except for a weak inhibitory effect on clone 13 (Fig.9). Furthermore, all clones had a weak activation of apoptosis, which was independent of the levels of STAT3β expression.

Judged by the intensity of the respective bands in the Western blot, the levels of STAT3β seemed to be much lower than those of STAT3α (Fig.14). Since STAT3β needs to heterodimerize with STAT3α to function as an inhibitor, STAT3β needs to be present in stoichiometric majority in order to bind all STAT3α molecules. Using COS cells transfected with STAT3α and different amounts of the β family member, it has been demonstrated that the transcriptional activity of STAT3α is partially inhibited using low amounts of DN-STAT3, but for complete inhibition, STAT3β needs to be

transfected at slightly higher levels than STAT3α, confirming that the wt molecule remains active in the case of insufficient expression of the DN (Caldenhoven *et al.* 1996). This could explain the lack of significant effects observed in proliferation and apoptosis when testing DU145-pVgRXR-pIND/hSTAT3β cells.

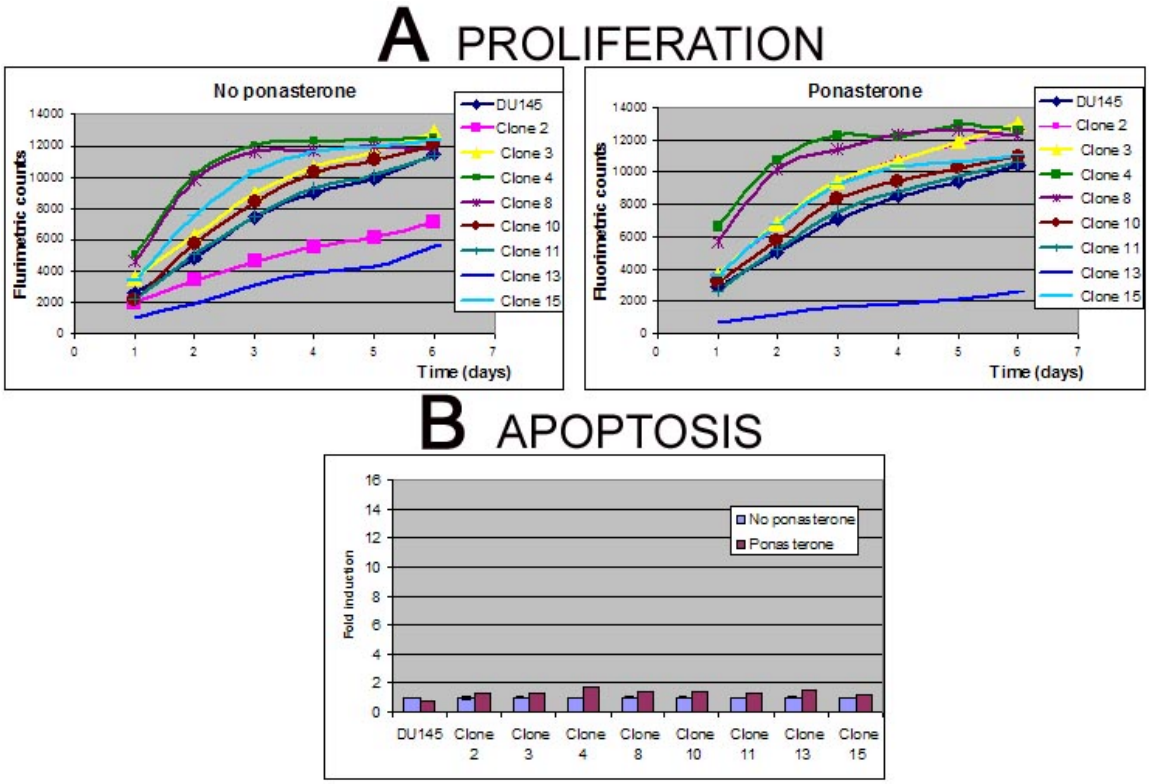

Fig.15. DU145-pVgRXR-pIND/hSTAT3β cells do not show changes in proliferation or in apoptosis in the presence (resp absence) of ponasterone. A) 3000 cells/well of either wt DU145 cells or DU145 cells stably transfected with pVgRXR and pIND/hSTAT3β were plated on a 96-well plate. When attached, ponasterone was added to a final concentration of 5 μM for the treated group. At the indicated time points, cell numbers were deduced by the measurement of mitochondrial activity using the AlamarBlue assay. B) 2000 cells/well of either wt DU145 cells or DU145 cells stably transfected with pVgRXR and pIND/hSTAT3β were seeded on a 384-well plate and, when attached, ponasterone was added to a final concentration of 5 μM for the treated group. At the indicated time points, apoptosis was measured by determination of caspase-3 activity. The fold induction was calculated setting the values of wt untreated cells as reference. Shown are the mean values and standard deviations of four measurements.

3.1.2.2. DN-STAT3 induction using the tetracycline system

3.1.2.2.1. Subcloning DN-STAT3 into a tetracycline inducible vector

Next it was attempted to reach higher levels of STAT3β using a tetracycline inducible system. The Flip-In T-Rex system was used for the generation of stable mammalian cells exhibiting tetracycline-inducible expression of a STAT3β from a specific

genomic location. To generate these cells, independent integration of a plasmid containing a Flp-recombination target (FRT) site (pFRT/LacZeo), and a plasmid expressing the Tet repressor (pcDNA6/TR) into the genome of the mammalian cell line of choice was required. After cloning and screening for LacZ reporter gene expression, to identify clones with integration of the pFRT/LacZeo plasmid into a high-expression site, the pcDNA5FRT/FRT/TO vector was introduced.

DN-STAT3 was amplified from pSG5 human-STAT3β vector, and a His-tag was introduced C-terminally by PCR primer mutation (Fig.16A). The product was then cloned into the pcDNA5/FRT/TO plasmid. Out of nineteen tested clones, two (clones 3 and 4) showed incorporation of STAT3β in the right orientation (Fig.16B). The results of the positive clones were confirmed by sequencing.

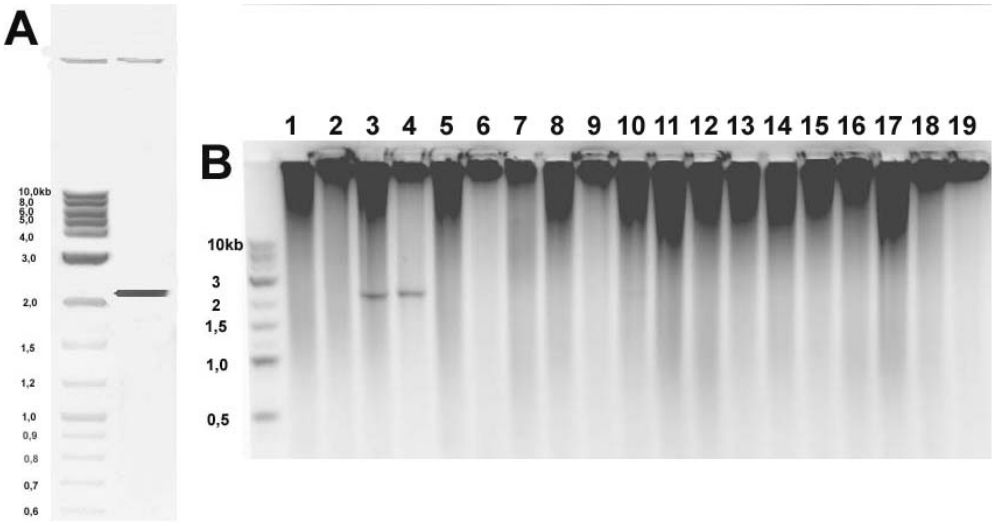

Fig.16. Sucloning of His-tagged human STAT3β into the pcDNA5FRT/TO vector. A) STAT3β was amplified from pSG5/hSTAT3β vector by PCR with 5'ATGGCCCAATGGAATCAGCTAC3' and 5'TCAGTGATGGTGATGGTGATGTTATTTCCAAACTGCATCAATGAATC3' as primers. The product was analyzed by DNA electrophoresis, and showed the right size. B) His-tagged human STAT3β was cloned into the pcDNA5FRT/TO vector, and nineteen clones were screened by PCR for incorporation and right orientation of DN-STAT3. The following primers were used: 5'ATGGCCCAATGGAATCAGCTAC3' and 5'TAGAAGGCACAGTCGAGG3'. Only clones 3 and 4 turned out to be positive.

5.1.2.1.2 Generation of stable DU145 Flip-In host cells (i.e. Du145 pFRT/LacZeo)

DU145 cells were transfected with pFRT/LacZeo and selected with 500 µg/ml zeocin during four weeks. Forty growing clones were expanded and tested for LacZ expression. A single clone was positive. However, this clone was growing very slowly, and the selection was stopped during two weeks. In the absence of antibiotic,

cells without plasmid expanded, and when tested for the expression of LacZ the culture was a mixed population of positive and negative cells (Fig.17).

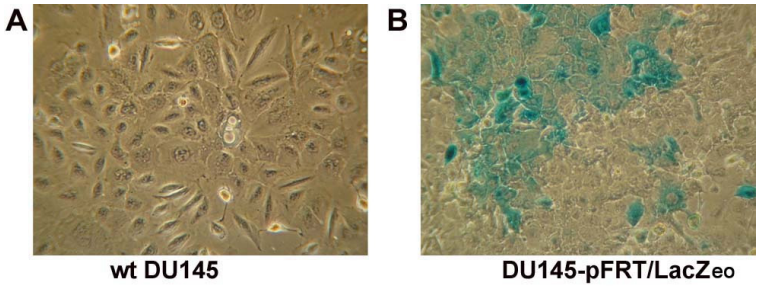

Fig.17. Identification of DU145 cells with stable incorporation of pFRT/LacZeo. $8x10^5$ cells/well were plated on a 6-well plate, and the following day assayed for expression of β-galactosidase by *in situ* staining.

5.1.2.1.3 Integration of the tetracycline repressor into DU145 Flip-In cells

The mixed population of DU145 Flip-In host cells was transfected with the pcDNA6/TR vector, and maintained under 500 µg/ml zeocin and 2.5 µg/ml blasticidin selection during three weeks. Under these conditions all cells died, and the same results were reproduced three times. This indicated either that none of the cells incorporated both plasmids, or that the selection conditions were too stringent.

5.1.2.1.4 Generation of tetracycline-inducible DN-STAT3 293 cells

293 cells with stable incorporation of pcDNA6/TR and pFRT/LacZeo were purchased from Invitrogen (293Trex cells). Since 293 cells had shown some response in the STAT3 RNAi experiments (see below), and they have been reported to produce tumors in mice (Graham 1987;Guan *et al.* 2001), they were chosen for the stable introduction of pcDNA5FRT/hSTAT3βHIS, to study the effects of STAT3 inhibition *in vivo*.

pcDNA5FRT/hSTAT3β-His and pOG44, a plasmid constitutively expressing the Flp recombinase, enzyme which recombines sequences flanked by FRT sites (Buchholz *et al.* 1996), were cotransfected into the 293Trex cells. Fifty hours after transfection, in order to let recombination take place, selection was started with 15 µl/ml blasticidin and 100 µg/ml hygromicin. The zeocin selection was removed, since the recombinant cells should have lost both the zeocin resistance and the LacZ gene. Once cells had been expanded, they were screened for the absence of LacZ. A uniform population

of 293 cells, which did not express LacZ, indicating pFRT/STAT3β-His incorporation, was identified (Fig.18).

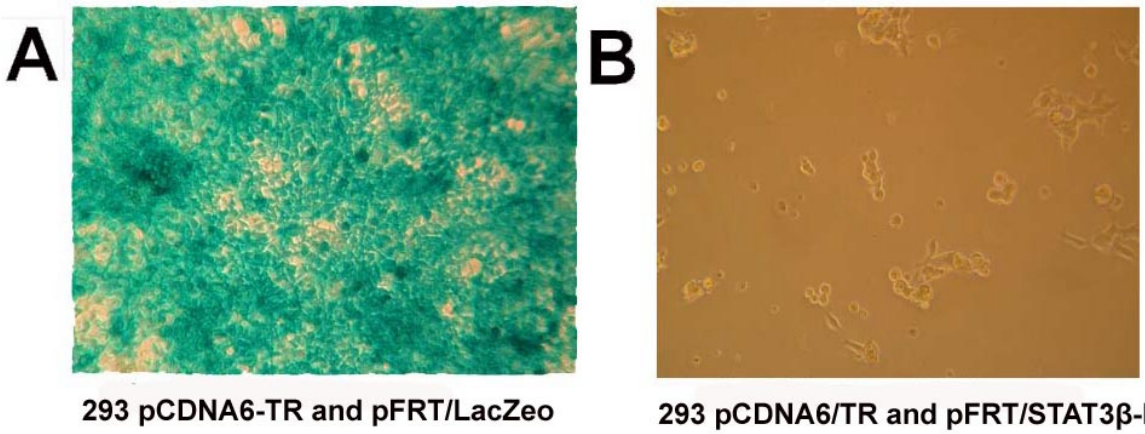

Fig.18. 293Trex cells with stable incorporation of pFRT/STAT3β-HIS do not express LacZ. 293Trex cells were cotransfected with pcDNA5FRT/hSTAT3βHIS and pOG44. 50 h after transfection, selection was started with 15 µl/ml blasticidin and 100 µg/ml hygromicin. The culture was expanded and tested for LacZ expression.

5.1.2.1.5 Tetracycline treatment of 293-pcDNA6/TR-pFRT/STAT3β-His cells induces the expression of STAT3β-His

In order to checks the expression of STAT3β-His in 293-pcDNA6/TR-pFRT/STAT3β-His cells, they were treated with 1 µg/ml tetracycline during several days. Both tetracycline treated 293Trex, and untreated 293-pcDNA6/TR-pFRT/STAT3β-His cells were used as controls. Only 293-pcDNA/TR pFRT/STAT3β-His cells showed expression of STAT3β-His.

Fig.19. 293-pcDNA6/TR-pFRT/STAT3β-His cells express STAT3β-His upon induction with tetracycline. 293-pcDNA6/TR-pFRT/STAT3β-His cells and 293Trex were treated with 1 µg/ml tetracycline for several days, or left untreated. Cells were harvested at the times indicated above, and the untreated cells were harvested with the latest group. Whole cell extracts were prepared, run on SDS-PAGE (10% polyacrylamide), and analyzed by Western blotting using an anti-His-tag antibody.

5.1.2.1.6 Tetracycline induction of STAT3β-His in 293-pcDNA6/TR-pFRT/STAT3β-His cells inhibits proliferation and induces apoptosis

STAT3β-His was induced in 293-pcDNA6/TR-pFRT/STAT3β-His, and the effects on proliferation and apoptosis were analysed. Three days after treatment with 1 µg/ml tetracycline, these cells showed a decreased proliferation, as compared to 293-pcDNA6/TR-pFRT/LacZeo, or untreated 293-pcDNA6/TR-pFRT/STAT3β-His cells. Furthermore, they showed activation of caspase-3, which started one day after treatment.

According to these results, blocking STAT3 in 293 cells induces the death of these cells, which is reflected by the decrease in proliferation and the activation of apoptosis.

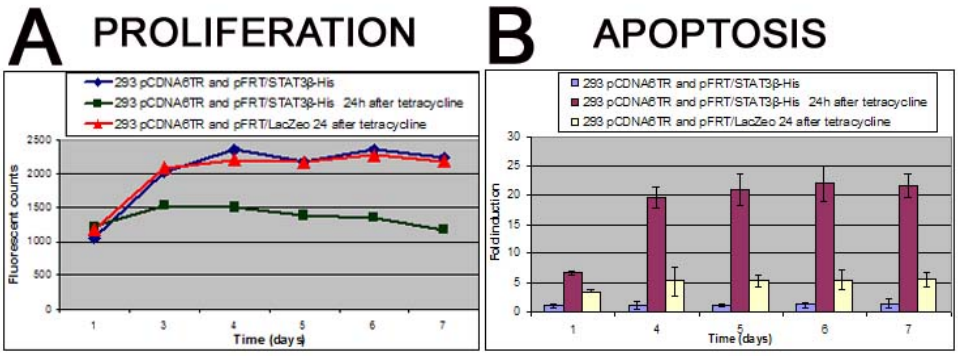

Fig.20. 293-pcDNA6/TR-pFRT/STAT3β-His cells show decreased proliferation and induction of apoptosis upon expression of STAT3β-His. A) 3000 cells/well of either 293 pcDNA6/TR-pFRT/STAT3β-His or 293-pcDNA6/TR-pFRT/LacZeo cells were plated on a 96-well plate, kept in full medium and treated with 1 µg/ml tetracycline, or left untreated. At the indicated time points, cell numbers were deduced by the measurement of mitochondrial activity using the AlamarBlue assay. B) 2000 cells/well of either MCF10A cells or MCF 10A cells stably transfected with v-Src were seeded on a 384-well plate and, several hours later, treated with 1 µg/ml tetracycline, or left untreated. At the indicated times, apoptosis was measured by determination of caspase-3 activity. The fold induction was calculated setting as reference the values of untreated 293-pcDNA6/TR-pFRT/STAT3β-His. Shown are the mean values and standard deviations of four measurements.

5.1.2.2 STAT3 inhibition using RNAi

The effects of STAT3 inhibition were also tested using another STAT3 inhibitory tool, in order to check whether the results were comparable in other experimental settings. Therefore, a STAT3 RNAi expressing vector (U6/STAT3i) was transiently transfected into v-Src MCF10A, DU145, and 293 cells. The levels of STAT3 were monitored

during forty hours (in the case of DU145 for up to 72 h). Only 293 cells showed a significant decrease of STAT3 40 h after transfection.

Fig.21. STAT3 can be inhibited in 293 cells using STAT3 RNAi. v-Src MCF10A cells, DU145 cells, and 293 cells were transfected either with pSilencer-1.0-U6 plasmid expressing the STAT3 RNAi pairs 5'AGUCAGGUUGCUGGUCAAAdTdT3' and 5'UUUGACCAGCAACCUGACUdTdT3', or with U6-empty vector. Untransfected cells were also used as a control. 40 or 72 h after transfection, cells were harvested, and whole cell lysates were prepared and analyzed by Western blot using a STAT3 antibody.

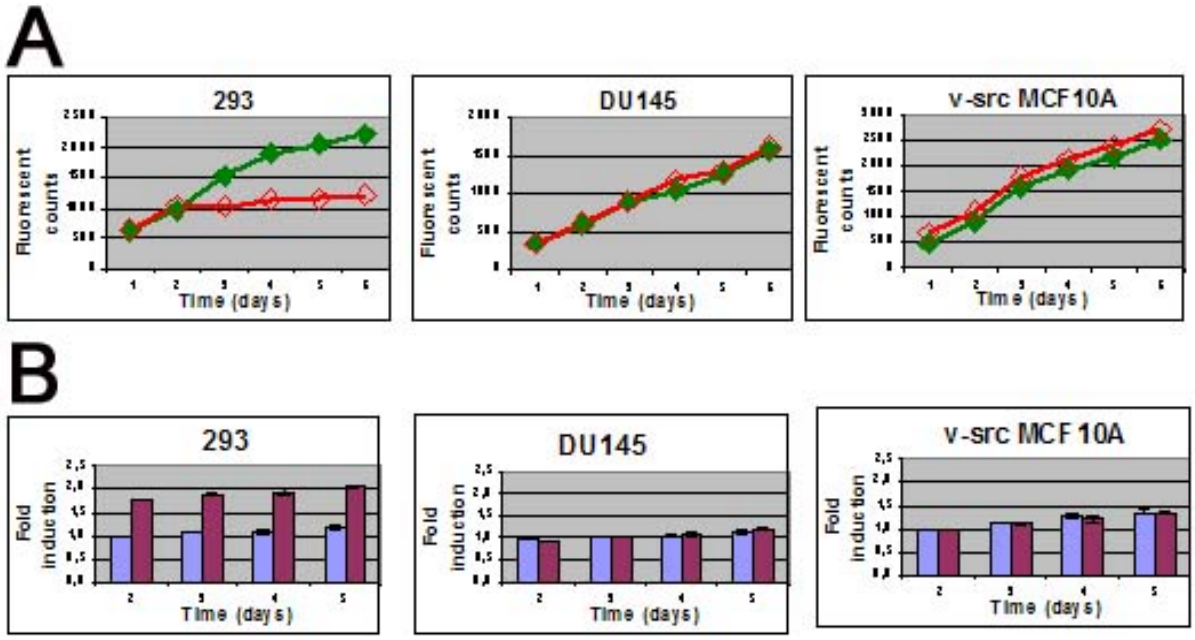

Fig.22. STAT3 inhibition using STAT3 RNAi induces apoptosis in 293 cells. MCF10A-v-Src-B3 cells, DU145 cells, and 293 cells were transfected either with pSilencer-1.0-U6 plasmid expressing STAT3 RNAi pairs, or with the empty vector. 24 h after transfection cells were seeded to test proliferation and apoptosis. A) 3000 cells/well were plated in a 96-well plate, and, when attached, maintained either in full growth medium, or starved. At the indicated time points, cell numbers were deduced by the measurement of mitochondrial activity using the AlamarBlue assay. Green shows proliferation in full medium, red under starved conditions. B) 2000 cells/well were seeded on a 384-well plate and, several hours later, either left untreated or starved. At the indicated time points, apoptosis was measured by determination of caspase-3 activity. The fold induction was calculated setting as reference the values in full medium of each respective cell line. Shown are the mean values and standard deviations of four measurements.

The effects on proliferation and apoptosis in the STAT3 RNAi treated cells were analyzed next. As mentioned above, MCF10A-v-Src-B3 and DU145 cells did not show any significant inhibition of STAT3 levels, and, consistent with these results, no

effect on proliferation or apoptosis was observed in these cells as compared to cells transfected with empty vector. This could reflect insufficient transfection efficiency. It is known that 293 cells are readily transfected, and this could explain why these cells were the only ones presenting a decrease in the STAT3 levels forty hours after transfection (Fig.21).

5.2 Pharmacological inhibition of STAT3

5.2.1 Definition of a pharmacophore for STAT3

5.2.1.1 Rational selection and *in silico* validation of STAT3 SH2-domain as a good target site

Both the SH2- and the DNA-binding domains of STAT3 might be good target sites for STAT3 inhibitors (see introduction). Therefore, the SH2 and DNA-binding domain were compared in the crystal structures of STAT3 (1BG1) and STAT1 (1BF5). These were downloaded from the protein data bank, and their properties were studied using ICM 2.8.

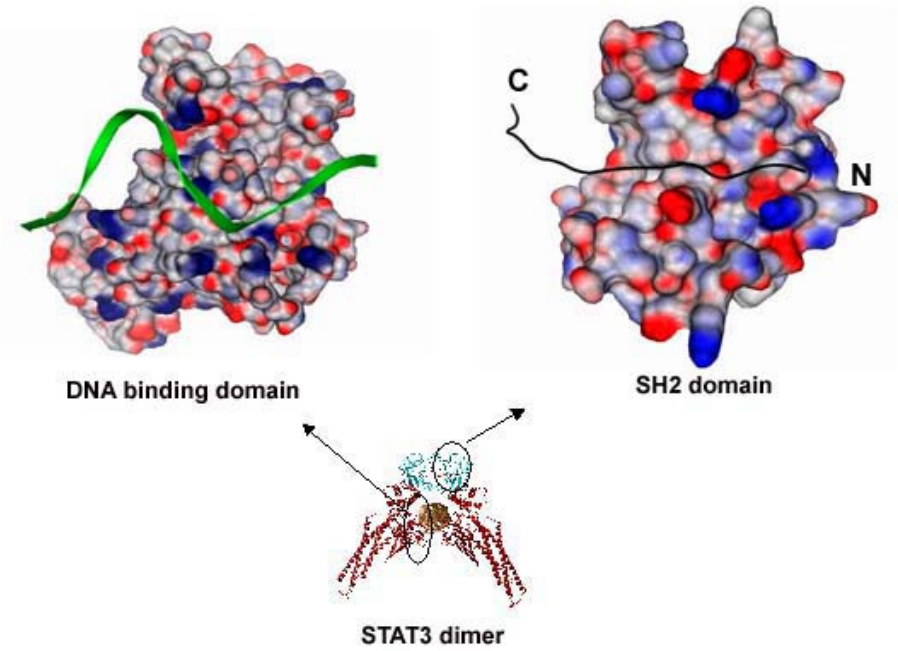

Fig.23. STAT3-crystal structure analysis. Shown is a surface representation of the DNA-binding- and the SH2-domains, contoured according to partial charge (red: negative; blue: positive). The DNA is represented as single-strand in green on the DNA-binding domain. The phosphotyrosine containing sequence is shown as black ribbon representation on the SH2-domain.

1BG1 and 1BF5 are the crystal structures obtained with mouse STAT3 and human STAT1, respectively. The human and mouse STAT3 family members are almost identical having just one substitution at the C-terminus (Asp^{760} for mice, and Glu^{760} for humans), which is part neither of the domains studied here, nor of the published structure. The mouse STAT3 crystal structure should therefore be identical to the human family member.

The dimeric form of STAT3 was generated *in silico* based on the monomeric unit published in the PDB data file (Fig.23). Then, the surface of the DNA-binding and SH2-domain were visualized, and the polarity in both parts of STAT3 was calculated in order to compare these regions with respect to their drugability. The analysis revealed that the SH2-domain had a profound pocket at the phospho-tyrosine interaction site, and that the polarity in this region was moderate. In contrast, the DNA-binding domain is very shallow, and highly positively charged (Fig.23). These results encouraged the selection of the SH2-domain as target site.

5.2.1.2 Proof of principle: blocking the SH2-domain inhibits STAT3 activity

In order to test whether blocking the STAT3 SH2-domain was sufficient to inhibit STAT3 activity, it was decided to use a phospho-STAT3-specific peptide. This STAT3 specific phosphotyrosine peptide was chosen based on the SH2-interacting region in STAT3 dimers (Fig.24). The sequence selected was AAPY*LKTK. The peptides were made cell penetrating with a sequence derived from antennapedia (RQIKIWFQNRRMKWKK) (Dunican and Doherty 2001), which was added N-terminally to the peptide. A biotin-tag was also placed at the N-terminus in order to enable their detection.

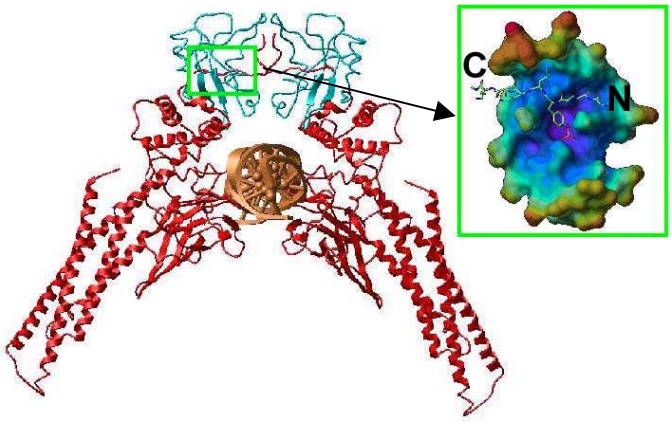

Fig.24. STAT3 dimer bound to the DNA. STAT3 crystal structure (1BG1) was downloaded from the PDB databank, and the dimer reconstituted based on the symmetry coordinates. The phosphotyrosine sequence of one of the monomers is highlighted in a green box.

Starved NIH3T3 cells were either incubated with cell-permeable and biotinylated AAPY*LKTK or left untreated. After one hour, they were tested by immunostaining for incorporation of the peptide, and it was found that they all had incorporated the antennapedia-tagged peptide (Fig.25).

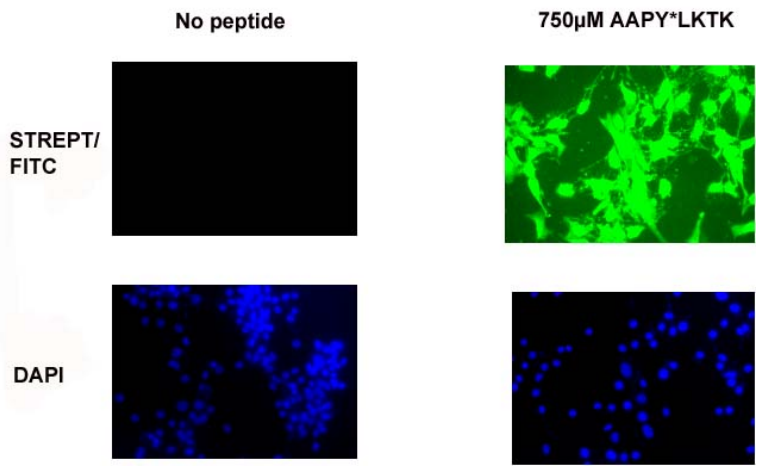

Fig.25. Antennapedia and biotin tagged AAPY*LKTK peptides penetrate into NIH3T3 cells within one hour. NIH3T3 cells were seeded on 6-well plates and starved overnight. The following morning, peptides were added to the treated cells, control cells were left untreated. One hour later, cells were harvested and stained in situ. The peptides were stained with streptavidin-fluoresceinisothiocyanate (FITC), and the nuclei with DAPI, as a control.

Next, the peptide was tested for its capacity to inhibit STAT3 activation in NIH3T3 cells. Cells were starved overnight, and since these cells had shown incorporation of the peptide after one hour, they were pre-treated for one hour with tagged AAPY*LKTK before adding interferonα/β (IFNα/β). The peptide turned out to inhibit IFNα/β-induced STAT3 activation (Fig.20A). However, the peptide had also a clear inhibitory effect on STAT1. This was not surprising, since STAT1 and STAT3 are known to heterodimerize. STAT3-specific peptides derived from the tyrosine containing sequence in STAT3 should consequently bind to both STAT1 and STAT3 SH2-domain. Furthermore, very similar results were reported by (Turkson *et al.* 2001) in studies using slightly shorter peptides.

As mentioned above, the SH2-domain is also required for recruitment of inactive STAT3 to the cytokine and growth factor receptors, where it then gets phosphorylated. Hence, it was hypothesized that blocking the SH2-domain could also inhibit phosphorylation of STAT3. This was tested next by Western blot, and it was found that the same conditions that enabled inhibition of STAT3 DNA-binding had no effect on STAT3 phosphorylation (Fig.20B).

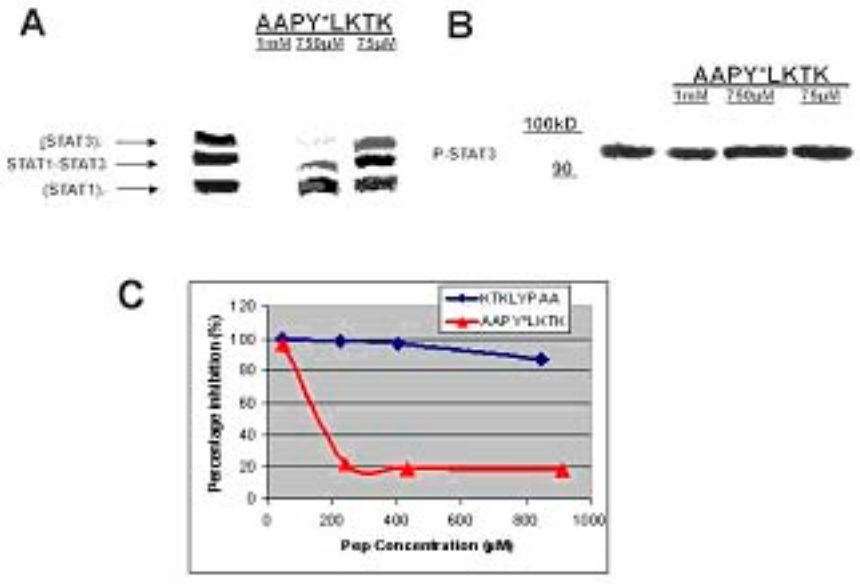

Fig.26. STAT3 specific phosphotyrosine peptides can block STAT3 de-novo dimerization, but they have no effect on STAT3 phosphorylation. AAPY*LKTK can disrupt STAT3 preformed dimers, too. A and B) $5X10^5$ NIH3T3 cells were seeded on a 6-well plate, and starved overnight. The following day, antennapedia and biotin-tagged AAPY*LTKT was added to the cells at the indicated concentrations. The control cells were left untreated during this step. One hour later, all cells were stimulated with 1000 units IFNα/β for 15 minutes. A) EMSA analysis of STAT1 and STAT3 using nuclear extracts B) phospho-STAT3 Western blot analysis using whole cell lysates. C) AAPY*LKTK and KTKLYPAA, the latter a scrambled peptide used as control, were incubated with nuclear extracts of NIH3T3-TKS3 cells for 30 min, and then assayed in the DNA-binding ELISA.

Finally, the peptides were tested for their capacity to disrupt preformed STAT3 dimers in a DNA-binding ELISA**.** Soluble and untagged AAPY*LKTK were incubated with nuclear extracts of NIH3T3-TKS3 cells, and assayed in the DNA-binding ELISA. KTKLYPAA was used as a negative control. AAPY*LKTK inhibited the DNA-binding of STAT3 with an IC_{50} of approximately 250 mM. Altogether, these results are consistent with the results published by Turkson *et al.* (2001), and indicated that inhibition of the SH2-domain could suffice for blocking STAT3 activity.

5.2.1.3 Selectivity: comparison with other SH2-domain containing proteins

Another important aspect to increase the chances of finding specific inhibitors for a molecule is the presence of unique structural features that differentiate it enough from other proteins in the cell. Therefore, the proteins sharing the highest similarity to the SH2-domain of STAT3 were searched, in order to predict if STAT3 specific inhibitors were feasible. A BLAST search was carried out with the protein sequence

of STAT3-SH2-domain versus the Humprot database, which contains all the human proteins from the SwissProt, TrEMBL, and PIR databases. It was found that the proteins sharing the highest homology were the members of the STAT family. In particular, STAT1 presented the highest homology level (59% identities), and was followed by STAT4, STAT2, STAT5, and STAT6 (Fig. 31).

PROTEIN	IDENTITIES	GAPS	SCORE	E-VALUE
STAT3 (P40763)	101/101	0%	183	3 e-47
STAT1 (P42224)	55/92	1%	114	2 e-26
STAT4 (Q14765)	50/91	1%	104	2 e-23
STAT2 (P52630)	46/91	1%	91	2 e-19
STAT5 A (P42229)	29/73	4%	59	1 e-9
STAT6 (P42226)	29/75	1%	59	2 e-9
STAT5 B (P51692)	29/73	4%	57	4 e-9

Fig.27. BLAST search of STAT3 SH2-domain (amino acids 570 to 670 of the P40763 sequence) versus 103164 sequences of human proteins published in Humprot database, using BLAST-P. The scores and E-values were calculated according to the Karlin-Altschul statistics (Schaffer *et al.* 2001;Altschul *et al.* 2001). The score depends on the length of the alignment and represents the degree of homology/similarity (higher scores represent better alignments). The E-value (Expectation value) represents the number of hits one can expect to find fortuitously when searching a database of a particular size.

As mentioned above, the crystal structure of STAT1, which is the protein presenting the highest homology to STAT3, has already been crystallized (Chen *et al.* 1998). This information was used in order to verify whether STAT1 and STAT3 presented structural differences that could enable specific inhibition.

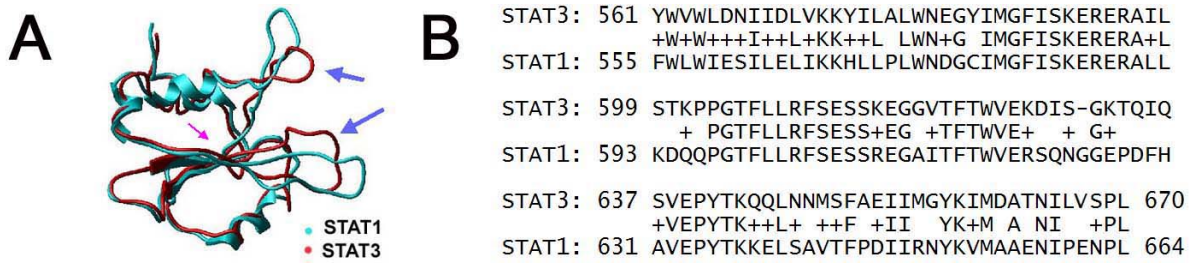

Fig.28. STAT1 and STAT3 SH2-domain comparison. A) Superimposition of human STAT1 (1BF5) on mouse STAT3 (1BG1) SH2-domain, as solved in the crystal structures. STAT1 and STAT3 present distinguished loops (indicated by blue arrows) that should enable the binding of compounds to just one of the molecules. The pink arrow indicates the phosphotyrosine-binding site. B) Aligned protein sequences of human STAT1 and STAT3 SH2-domain. Conservative substitutions are marked by a +.

Visualized upon superimposition of both proteins, the SH2-domains shared a very similar general structure. However, some loops in the crystal structures presented a different disposition (Fig.28A).

A

PROTEIN	IDENTITIES	GAPS	SCORE	E-VALUE
STAT3 (1BG1)	101/101	0%	182	2 e-47
STAT1 (1BF5)	60/101	0%	40	3 e-27
Src (e.g. 1A09)	15/35	2%	28	0.77
RHODOPSIN (e.g. 1LN6)	17/48	16%	27	1.6
FYN (e.g. 1AOT)	14/26	3%	26	2.4
Calmodulin sensitive adenylate cyclase (e.g. 1K93)	21/84	27%	26	3.5
Results second run:				
BLK (e.g. 1BLJ)	23/58	10%	29	0.3
Penicillopepsin (e.g. 1PPL)	17/57	5%	29	0.43
Phosphatidylinsositol 3-kinase (e.g. 2PNB)	13/36	0%	26	3.0
SAP (e.g.1KA6)	14/28	3%	26	3.1

B

```
 Identities = 15/35 (42%), Positives = 22/35 (62%), Gaps = 1/35 (2%)

human STAT3: 12 EGYIMGFISKERERAILSTKPP-GTFLLRFSESSK 45
                E Y      +E ER +L+ + P GTFL+R SE++K
human c-src: 7  EWYFGKITRRESERLLLNAENPRGTFLVRESETTK 41
```

Fig.29. BLAST analysis of STAT3 SH2-domain using the BLAST-PSI software versus 36110 sequences of human proteins published in the PDB database. A) The scores and E-values were calculated according to the Karlin-Altschul statistics (Schaffer *et al.* 2001;Altschul *et al.* 2001). S depends on the length of the alignment and represents the degree of homology/similarity (higher scores represent better alignments). The E-value (Expectation value) represents the number of hits one can expect to find fortuitously when searching a database of a particular size. The values obtained in the second run are calculated with modified statistical parameters (Schaffer *et al.* 2001), and can therefore not be compared to the values obtained in the first run. B) Alignment of human STAT3 and human c-Src. Conservative substitutions are marked by a +.

Next, other crystallized proteins presenting some similarity to STAT3 SH2-domain were searched, in order to compare them and study potentially conserved characteristics. Therefore, a BLAST search of STAT3-SH2-domain versus the PDB database was performed. STAT1 was the only similar protein but other SH2-domain containing proteins, such as Src, showed some degree of homology, although very remote. However, it was found that over a stretch of 35 amino acids in the case of Src, 15 amino acids are identical to STAT3 (Fig.29). Something similar was observed with the other proteins. Since these residues were conserved in many SH2-containing proteins, it was theorized that they could be important for the function of these domains, and were therefore studied next in the crystal structures.

5.2.1.4 *In silico* selection of specific residues in the STAT3 SH2-domain as promising pharmacophore

A number of crystal structures of Src are available in the PDB, and some of these proteins belong to different species, but they all share identical sequence at the phospohtyrosine binding site. Only the ones solved with a resolution of <2.2 Å were used to perform a structural comparison of their SH2-domains with STAT1 and STAT3. The following Src structures were selected for the analysis: 1A09, 1 hCS, 1 hCT, 1A07, 1A08, 1A1E, 1A1B, 1A1C, 1A1A, 1FMK, 1SHD, 2SRC, 1QCF1SHB, 1SHA, 1F1W, 1F2F, 1SPR, 1IS0, 1SKJ, 1KC2, 1BKL, and 1BKM.

The structural properties of STAT3 were compared to all these SH2-domain containing proteins using the SwissPDBViewer software. Superimposition of STAT1 and these Src structures on STAT3 revealed some identical, and many different features. The overall structure of STAT3 and STAT1 were quite distinct from all Src structures, but the phosphotyrosine-binding site matched very well in all of them, and corresponded to the region identified in the BLAST searches, which shares high similarity at the protein sequence level (Fig.29). However, the structures differed considerably in the regions that bind to the amino acids C-terminal of the phosphotyrosine (Fig.30A).

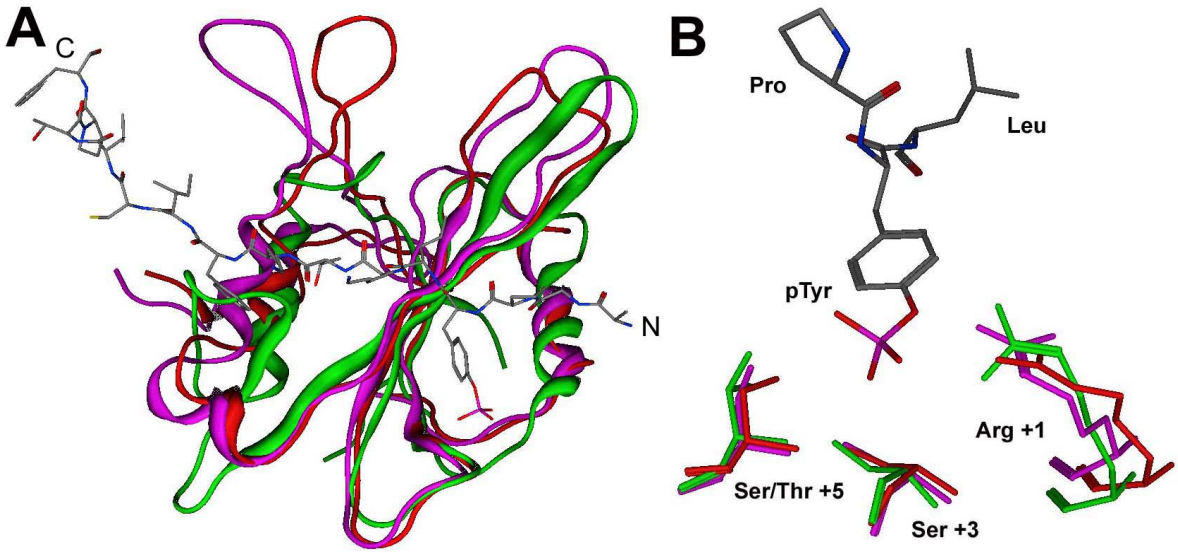

Fig.30. Superimposition of human STAT1 (1BF5, magenta), and c-Src (1F1W, green) on mouse STAT3 (1BG1, red). A) SH2-domain. B) conserved residues (Arg 609, Ser 611, Ser 613). Note the different orientation compared to (A). Magenta STAT3, green superimposed structures.

A closer look revealed a highly conserved interaction of the phosphotyrosine (residue 705 in the case of STAT3) with three residues in the SH2-domain: an Arg (Arg^{609} for STAT3), a Ser (Ser^{611} for STAT3), and another Ser (Ser^{613} for STAT3), the latter sometimes substituted by a Thr in some of the proteins (Fig.30B and 31). Arg^{609}, Ser^{611}, and Ser^{613} of STAT3 superimposed very closely with the corresponding Arg^{X}, Ser^{X+2}, and Ser/Thr^{X+4} residues of all the other structures with a Root Mean Square (RMS) smaller than 1.6 Å (Fig.30.B). Otherwise, the folding of the SH2-domains of Src and STAT SH2-domains did not match. Only STAT1 presented additional conserved residues with STAT3. These amino acids were involved in interactions at the binding site for the phosphotyrosine and its C-terminal sequence. Some of the interactions, however, were specific for each STAT protein, and were only found in STAT1 or STAT3 (Fig.31)

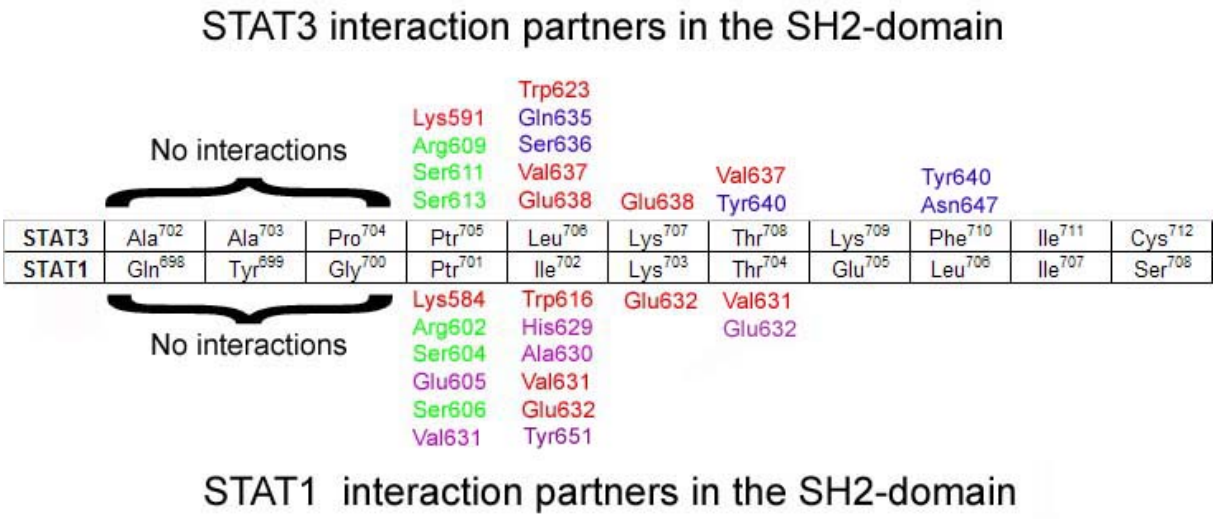

Fig.31. Overview of the interactions of the phosphotyrosine containing sequences of STAT1 and STAT3 with the corresponding SH2-domain. The sequences in the center correspond to the phosphotyrosine-containing sequences of STAT3 (top), and STAT1 (bottom). Residues listed above (for STAT3), or below (for STAT1) each residue of the phosphotyrosine-containing sequence, represent the interaction partners in the SH2-domain that interact at a distance of up to 4Å. Residues highlighted in green indicate polar interactions conserved in all SH2-domains, in red interactions conserved in STAT1 and STAT3, in blue interactions important only in STAT3, and in pink interactions important only in STAT1.

This structural analysis indicated that most of the interactions at the SH2-domain of STAT1 and STAT3 were different, but that both molecules shared some important interactions, especially at close proximity of the phosphotyrosine-binding site. Expanding the pharmacophore C-terminally of this region should enable specific inhibition of STAT3.

In conclusion, STAT1 turned out to be the protein sharing the highest similarity with STAT3 at the sequence and structure level. Still, it presented some distinct features that could permit the development of specific inhibitors.

5.2.2 STAT3 dimerization assay: ELISA

Next, a dimerization assay for STAT3 was required to test compounds with medium throughput. In order to test for compounds that specifically block the SH2-domain, so far, two assays are described in the literature:

1. A pull-down assay, involving the binding of non-phosphorylated STAT3 to bead-coupled, phosphorylated, STAT3-specific peptides (Turkson *et al.* 2001),
2. An EMSA-based assay, which detects the binding of phosphorylated, dimerized STAT3 to the DNA (Turkson *et al.* 2001).

Both assays can be used to test small amounts of molecules, but they are hardly applicable for medium- or high-throughput purposes. The second assay can be used as an ELISA-type assay, as described in Materials and Methods. Yet, like the EMSA assay, it has the drawback of not being able to discern dimerization blockers from DNA-binding inhibitors. Attempts to establish assays using the purified SH2-domain to perform ELISA type assays (Haan *et al.* 1999), or Biacore assays (unpublished data) only functioned at acidic pH. Under these conditions the folding and binding properties could differ from the ones that take place physiologically. Therefore, a new assay was developed.

5.2.2.1 Streptavidin-based ELISA

Initially, the assay was conceived as follows (Fig.32):

1. Coating of streptavidin coated 96-well plates with biotinylated, phosphorylated STAT3-specific peptides
2. Binding of non-phosphorylated, human, recombinant STAT3 protein
3. Detection of STAT3 protein with STAT3-specific antibodies
4. Binding of HRP-labeled secondary antibody
5. Development of the signal using colorimetric reagents

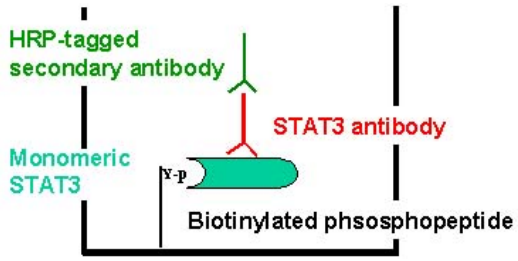

Fig.32. Streptavidin-based STAT3 dimerization assay principle: Biotinylated-STAT3-specific phosphopeptide bound on streptavidin-coated plates is recognized by monomeric STAT3. Detection is achieved by a STAT3 specific antibody, and the signal is provided by a horseradish-peroxidase-labeled secondary antibody.

For the assay, human recombinant STAT3 and c-Src were produced in insect cells (kindly provided by Dr. Uwe Hofmann, Merck Darmstadt), and whole cell lysates were prepared. The levels of expression of the proteins were validated by Western blotting (Fig.33).

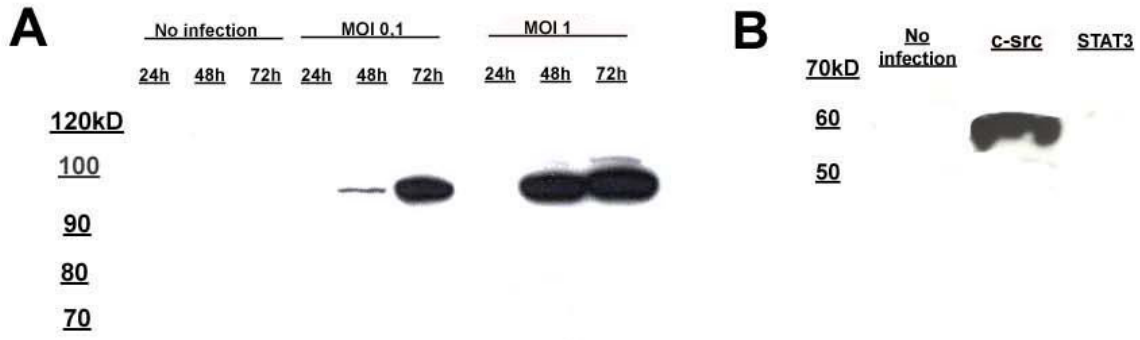

Fig.33. STAT3 and c-Src expression in SF9 cells. A) High expression of STAT3 in Sf9 cells is achieved 48 h after infection. A suspension culture of Sf9 cells was infected with STAT3 baculoviruses at the indicated MOI, harvested at the indicated time points, and lysed in 1% NP40 lysis buffer. Uninfected cells were used as negative control. Expression of STAT3 was tested by Western blotting using the Penta-His antibody B) C-Src expression in c-Src infected Sf9 cells. Sf9 cells were infected with c-Src baculovirus, harvested 48 h after infection, and treated as described in A). C-Src was detected using a Src specific antibody (controls: uninfected cells, and STAT3 expressing cells).

Next, C-terminally-biotinylated phospho-STAT3-specific peptides, derived from the phosphotyrosine sequence as described before, were coated on streptavidin-coated 96-well plates. The coating of the biotinylated peptides (AAPY*LKTKFK-biotin and PY*LKTKK-biotin; FKTKLYPAAK-biotin as negative control) was verified with an anti-phospho-STAT3-antibody, and it was found that using 5 ng of peptide sufficed to saturate the surface (Fig.34A).

Once the coating of streptavidin-coated plates with biotinylated phospho-STAT3 peptides had been achieved, the insect cell lysates were tested in the ELISA. C-Src and non-infected Sf9 cell lysates were used as a control. However, both gave similar signals to the STAT3 extracts. Additionally, no difference in the binding to the specific

and irrelevant peptides could be obtained. Altogether indicated that the assay was not measuring the STAT3-SH2-domain interaction with the phospho-peptide, and that the background of the assay under these conditions was very high. Different blocking reagents, such as milk, casein, BSA, and some commercial solutions were tested, but none decreased the background sufficiently.

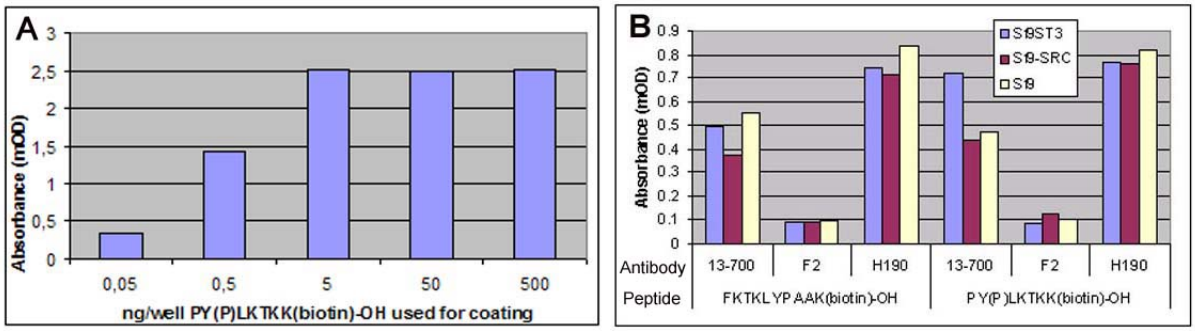

Fig.34. No specific signal of STAT3 binding to phosphotyrosine peptides using the biotin-streptavidin based ELISA. A) Using 5 ng of biotinylated-phospho-STAT3-specific peptide per well is sufficient to saturate the coating capacity of streptavidin-coated plates. Biotinylated PY*LKTK peptide was coated on the plates, and detected with phospho-STAT3 specific antibody. B) Testing of different STAT3 specific detection antibodies. Cell lysates of Sf9 cells infected with STAT3-, Src- expressing baculovirus, and uninfected Sf9 cells were tested in the streptavidin based ELISA as described in Fig.32. Peptides PY*LKTK or FKTKLYPAA, the latter as control, were coated on the plates, and detection antibodies used in each case are indicated.

5.2.2.2 Flag-tag based ELISA

It was found that STAT3 could be pulled down by streptavidin-coated peptide beads (personal communication of James Turkson and Ralph Buettner). Since streptavidin seemed to be presenting affinity for STAT3, it was decided to tag the peptides with the Flag-tag peptide (DYKDDDDK), and the assay was performed as follows:

1. Coating of 96-well plates with anti-Flag-tag antibody
2. Capture of Flag-tagged, phosphorylated STAT3-specific peptides
3. Binding of non-phosphorylated, human, recombinant STAT3 protein
4. Detection of STAT3 protein with STAT3-specific antibodies
5. Binding of HRP-labeled secondary antibody
6. Development of signal using colorimetric reagents

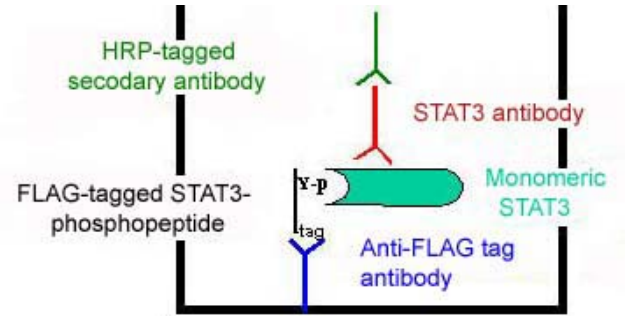

Fig.35. Flag-tagged based STAT3 dimerization assay principle: FLAG-tagged-STAT3-specific phospho-peptide bound on anti-Flag antibody-coated plates, is recognized by monomeric STAT3. Detection is achieved by a STAT3 specific antibody, and a horseradish-peroxidase-labeled secondary antibody provides signal.

5.2.2.2.1 STAT3 binds to phosphorylated STAT3 peptide

Under these conditions, only STAT3 gave a significant signal, whereas with the negative control (c-Src containing cell-lysates) no signal was obtained. Furthermore, STAT3 only bound to the phosphopeptide, not to the control (Fig.36).

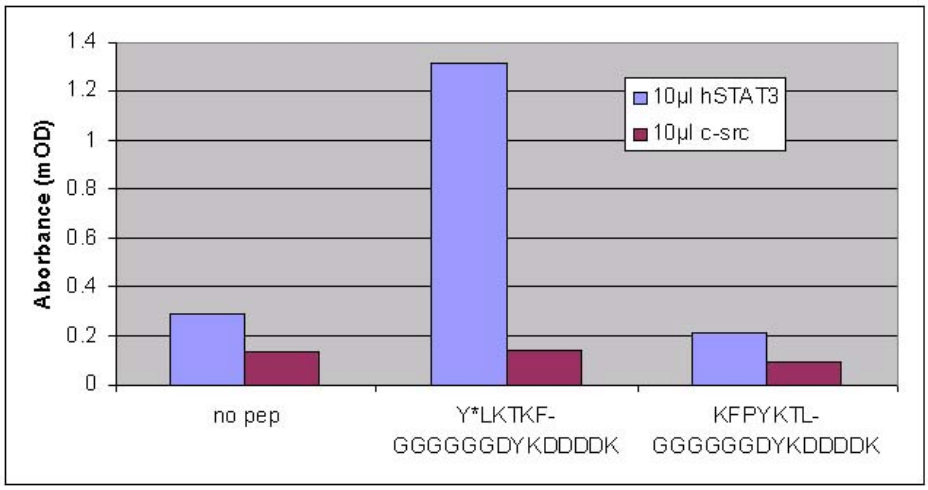

Fig.36. Specific detection of STAT3 bound to phosphorylated STAT3 peptide. Human STAT3 and c-Src were expressed in Sf9 cells, and whole cell lysates were prepared and tested in the Flag-tag based ELISA. C-Src, and the scrambled peptide (KFPYKTL) were used as negative controls.

Once a specific signal had been achieved, the assay conditions were optimised in order to get the best signal to noise ratio. Different blocking agents, buffers, and antibodies were tested in order to diminish the background. The optimal conditions established for this assay are described in Materials and Methods.

5.2.2.2.2 Soluble STAT3 specific peptides compete with Flag-tagged peptides for STAT3 binding, non-related peptides do not

The phosphotyrosine-peptide/SH2-domain interaction is highly precise, and this selectivity is very important in biological systems in order to enable binding only to specific signaling molecules. The sequence C-terminal of phosphotyrosines mediates very specific interactions which allow the many SH2-domain containing proteins in a cell to discern and bind to a single, or a few tyrosine-phosphorylated proteins (Cantley and Songyang 1994;Williams *et al.* 1991;Zvelebil *et al.* 1995).

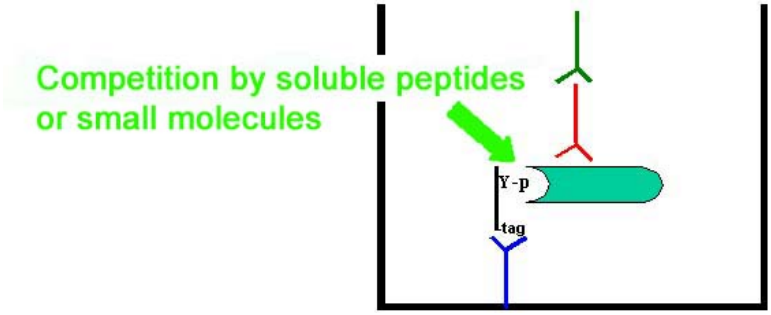

Fig.37. Competition assay principle: preincubation of monomeric STAT3 with peptides or small molecules that bind to the SH2-domain should inhibit the signal obtained in the Flag-tagged based dimerization assay.

Proper folding of non-phosphorylated STAT3 could not be verified through a Western blot analysis, but only through structure-elucidating studies using nuclear magnetic resonance, or mass-spectroscopy of its crystals, both of which were not feasible at this point of the study. Instead, an indirect test, based on competition experiments (Fig.37), was performed to verify that the specificity of the interaction was tight.

STAT3 specific and non-specific peptides derived from different proteins, such as SMAC, a caspase activator, TIE2, a tyrosine kinase, and other STAT3-dimerization-irrelevant sequences were preincubated with recombinant STAT3, before adding the STAT3-Flag-tagged peptide. The ELISA was then continued as described in Materials and Methods. Only phosphorylated, STAT3-specific peptides were able to disrupt the binding to the Flag-tagged peptide (Fig.38).

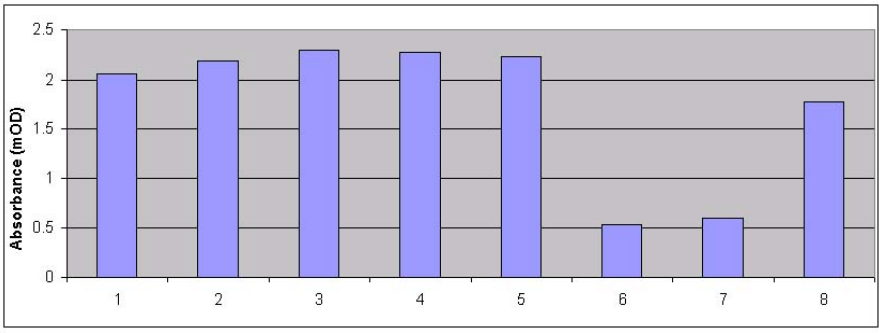

1	No peptide	
2	SMAC peptide[a]	AVPIAQK-Biotin
3	Tie-2 substrate[b]	Biotin-Aca[c]-LEARLVAYEGVVVAGK
4	Phosphorylated Tie-2 substrate	Biotin-Aca-LEARLVAY*EGVVVAGK
5	Scrambled, non-phosphorylated STAT3	FKTKLYPAA
6	Phosphorylated STAT3 peptide	AAPY*LKTKFK
7	Phosphorylated STAT3 peptide	AAPY*LKTKFK-Biotin
8	Scrambled, non-phosphorylated STAT3	FKTKLYPAAK-Biotin

a Sequence derived from SMAC protein; activator of apoptosis
b Substrate peptide of the tyrosine kinase Tie2 (angiopoeitin receptor; inhibitor of angiogenesis
c Aca stands for ε-aminocaproic acid, used to bind the biotin tag

Fig.38. Only phosphorylated STAT3 specific peptides are able to disrupt binding of monomeric STAT3 to Flag-tagged phospho-STAT3 peptide coated plates. STAT3 containing Sf9 cell lysates were preincubated with the indicated peptides at 1 mM, and then tested in the FLAG-tag based ELISA.

5.2.2.2.3 The Flag-tag based ELISA enables relative quantification of non-phosphorylated STAT3, and of the potency of SH2 inhibitors

Since ELISAs are quantitative assays, the capacity of the present assay to reflect different amounts of STAT3 was evaluated. This was verified using 1 to 50 µl insect cell lysates, which had a total protein concentration of 5.7 µg/µl. The signal obtained formed a sigmoid curve (Fig.39A), with a detection limit and a saturation point, typical of quantitative signals. In this case, the detection limit was reflecting the smallest amounts of STAT3 capable of giving a measurable signal, and, at saturation, the anti-Flag-tag binding sites on the plate had maximal occupancy. Surprisingly, using too much of the protein extracts decreased the signal. This was repeatedly observed, and might reflect the presence of 1% NP40 detergent in the lysates, which, when not diluted enough, could be washing away the bound proteins from the assay.

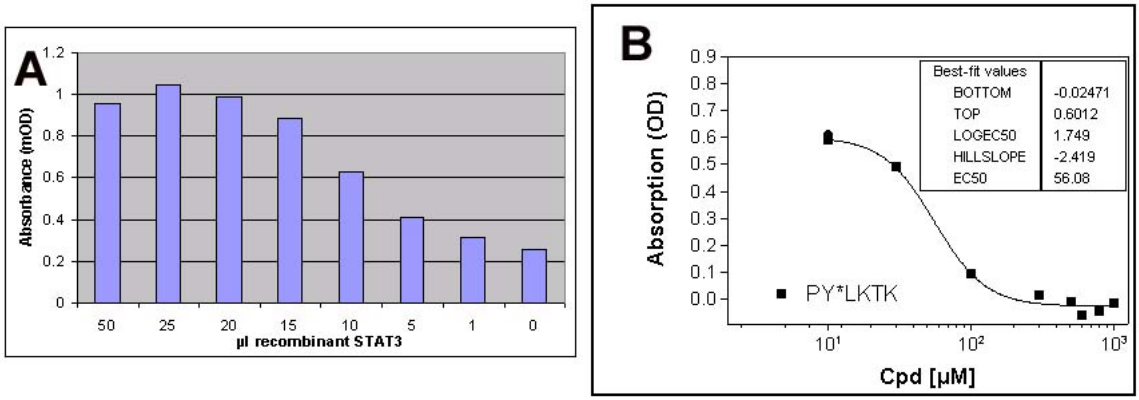

Fig.39. Flag-tag based ELISA as an assay for STAT3 dimerization inhibitors. A) Determination of relative amounts of recombinant STAT3 in cell lysates. Different amounts of Sf9-STAT3 cell lysates were tested in the Flag-tag ELISA. B) Determination of the IC_{50} of dimerization inhibitors. 15 µl of non-phosphorylated Sf9-STAT3 cell lysates were preincubated with different amounts of peptide PY*LKTK for 30 min, and then tested in the Flag-tag based ELISA. The concentration of peptide was calculated for the final assay volume, i.e. 100 µl.

As presented above, the STAT3 signal could be competed with peptides. The capacity to titrate this inhibition was of importance, since this would allow quantifying the potency of SH2-binders. For competition, concentrations of 10 to 1000 µM of peptide PY*LKTK were tested. Again, the characteristic sigmoid curve was obtained, confirming the quantification ability of this assay (Fig.39B).

5.2.2.2.4 Robustness of Flag-tag ELISA

In order to use an assay for the comparison of many compounds it is necessary to assess its stability and robustness, i.e. that the signals obtained in replicates and in repeated experiments are statistically equivalent. In order to confirm to confirm that this was the case with the established STAT3 dimerization assay, a z-test was performed. In three separate experiments performed on different days, the signal obtained with 15 µl STAT3 lysate (positive control), and by competition with 500 µM PY*LKTK were measured in eight repeats. The standard deviations (SD), the mean values (Mean) and the Z-value (formula follows) were calculated for each separate experiment.

$$Z=1-(3XSD_{PosCon} + 3XSD_{NegCon})/(Mean_{PosCon} - Mean_{NegCon})$$

Z-factors between 0.5 and 1.0 indicate excellent assay quality. 0.671, 0.555 and 0.663 were obtained for the three tests. Consequently, this ELISA was giving significant and reproducible results, and was suitable for compound screenings.

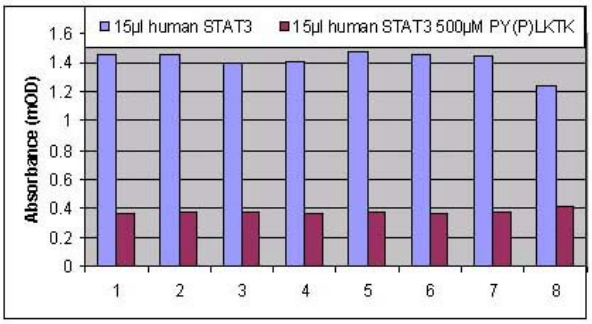

	No peptide	PY(P)LKTK	%Percent control
	1.450	0.367	15.317
	1.449	0.368	15.359
	1.395	0.368	15.359
	1.406	0.360	15.025
	1.470	0.368	15.359
	1.451	0.366	15.275
	1.447	0.370	15.442
Mean	1.235	0.412	17.195
SD	0.076	0.016	0.180
Z value	0.663		

Fig.40. Statistical significance of inhibition of STAT3 binding to Flag-tagged peptides, by competition with soluble peptides. Untreated STAT3 Sf9 cell extracts, and the same extracts pretreated for 30 min with peptide PY*LKTK were tested in the Flag-tag based ELISA. Each group was tested in eight repeats, and the same experiment was repeated three different days. The z-value, which is a measure of the signal to noise ratio, was calculated by $Z=1 - (3XSD_{PosCon} + 3XSD_{NegCon})/(Mean_{PosCon} - Mean_{NegCon})$. The assay was considered robust when Z>0.5. The obtained values in the three repeated experiments were 0.671, 0.555 and 0.663.

5.2.3 Evaluation of structural observations and predictions

Using the established STAT3 dimerization assay, it was possible to test the relevance of the observed interactions taking place between the phosphotyrosine containing sequence and the STAT3 SH2-domain.

5.2.3.1 Peptide predictions

First, a number of STAT3-specific phosphotyrosine containing peptides, varying in length and including some Ala-mutants, were tested in this assay (Table 1). In the crystal structure of dimeric STAT3, residues 702 to 712, which are surrounding the phosphotyrosine 705, are not very far from the SH2-domain. But a closer analysis revealed that the amino acids, which are N-terminal of the phosphotyrosine (Ala^{702}, Ala^{703} and Pro^{704}), did not undergo any direct interactions with the SH2-domain. Two other studies using STAT3-specific peptides have been published. The work done by (Turkson *et al.* 2001) indicated that occupation of position –1 of the phosphotyrosine was necessary for the binding of phosphopeptides to the SH2-domain. However, the

peptides tested by Ren *et al.* (2003), and the observation made in the present work, indicated that Pro^{704} did not interact directly with the SH2-domain in the dimer (Fig.31). Therefore, different peptides with and without the Pro were tested in the dimerization assay. Peptides Y*L, Y*LK, Y*LKT, and Y*LKTK all bound to STAT3, with IC_{50} values of 66, 63, 40 and 31 μM, respectively. However, peptide PY* did not show inhibition at the tested concentrations (i.e. up to 1 mM). These results did not confirm the essential role of position –1, nonetheless, peptides PY*L, PY*LK, PY*LKT, and PY*LKTK, generally showed a slightly increase in affinity (68, 45, <14, and 15 μM, respectively), as compared to the non-Pro containing ones. Altogether indicated that position –1 was not essential for the binding of phospho-peptides to STAT3, but that residues occupying this position could interact with the SH2-domain, which increased the affinity of the peptides slightly. In the dimer, the Pro at this position might not be undergoing interactions with the SH2-domain, not only because the pocket at this site is not very profound, but maybe due to the structural constraints at the phosphotyrosine containing sequence, which in STAT3 dimers is part of a long protein chain. In a STAT3 protein, the phosphotyrosine containing sequence certainly must have some flexibility, but might not be able to move as freely as peptides. One could argue accordingly about positions –2 and –3, but elongation of peptide PY*LKTK (IC_{50} 15 μM) at these positions did not increase affinity (peptide APY*LKTK and AAPY*LKTK 27 and 21 μM, respectively). This might be reflecting the presence of a pocket at the Pro-binding site that is not optimally occupied in the dimer, as opposed to further N-terminal positions, where no binding sites seem to be able to contribute to binding.

The analysis of the crystal structure revealed interactions between the phosphotyrosine containing sequence and the SH2-domain, starting at the phosphotyrosine and up to Thr^{710}. Turkson *et al.* (2001) reported the critical role of Leu^{706}, and according to the studies published by Ren *et al.* (2003) this amino acid enables optimal binding to the SH2-domain. In the present work, the pocket involved in the binding of Leu^{706} was defined as formed by Trp^{623}, Gln^{635}, Ser^{636}, Val^{637}, and Glu^{638} (Fig.31). As opposed to Pro^{705}, Leu^{706} contributes to the affinity of the interaction in a significant way. This observation was confirmed by the results obtained with the peptides: Y*L was the minimal peptide showing inhibition in the dimerization assay, with an IC_{50} of 66 μM, and substitution of this amino acid by an

Ala in peptide Y*LKT, decreased the affinity significantly (Y*LKT 40 µM, vs. Y*AKT 490 µM).

It was observed that after Leu^{706} only every second residue bound with its side chains to the SH2-domain. Lys^{707} only interacted with its backbone to Glu^{638}, and it did not bind to a pocket, rather, the binding to the SH2-domain was superficial. In this case, this would be in line with the findings of Turkson *et al.* (2001), which indicated that this position is not essential for binding. Indeed, adding this residue to peptide Y*L did not increase the affinity significantly (Y*L 66 µM vs. Y*LK 63 µM), and mutation of this residue in peptide Y*LKT (40 µM) did even slightly increase the affinity (Y*LAT 21 µM).

According to the interactions studied in the crystal structure, Thr^{708} contributed significantly to the binding of the phosphotyrosine containing sequence. Turkson *et al.* (2001) did not study positions downstream of Y^{+2}. In the dimerization assay, addition of position + 2 to peptide Y*L did not change affinity, and position + 3 increased the affinity slightly (Y*L 66 µM, and Y*LK 63 µM vs. Y*LKT 40 µM). However, substitution of this amino acid by an Ala in peptide Y*LKT did not affect binding significantly (Y*LKT 40 µM vs. Y*LKA 31 µM). The structural analysis had revealed that Thr^{708} only bound to two amino acids (Val^{637} and Tyr^{640}), while Leu^{706} bound to a pocket involving five residues (Fig. 35).

These results would support the model that only Leu^{706} was binding optimally in STAT3 dimers, and that Thr^{708} contributed to dimerization only weakly. Ren *et al.* (2003) published the sequence of a high-affinity STAT3 peptide, which has a Gln instead of a Thr at position + 3, but a Gln. This supports that the pocket at position + 3 is not optimally occupied by a Thr, and that this position could be leveraged to improve the affinity of peptides to the SH2-domain.

Altogether, the studies performed with the peptides confirmed the importance of position + 1 of the phosphotyrosine to interactions with the SH2-domain, and showed that binding at position –1 is not essential, but enables interactions that can increase the peptide affinity. Finally, position + 3 was shown to be contributing to binding. Accordingly, out of the tested compounds, peptide PY*LKT had the best affinity <14 µM. However, it could be expected that substitution of the Thr by a Gln could still improve the binding.

680 EAFGKYCRPESQEHPEADPGSAAPY*LKTKFICVTPTTCSNTIDLPMSPRA 730

Sequence	%Control at 1mM		IC50(μM)	
	Exp.1	Exp.2	Exp.1	Exp.2
PY*	76	72	>1mM	>1mM
Y*L	1	1	43	88
APY*	116	102	>1mM	>1mM
PY*L	1	-2	73	62
Y*LK	2	-1	60	66
Y*LAT	1	-2	23	19
Y*AKT	25	35	570	410
Y*LKA	3	0	26	35
PY*LK	4	-1	39	50
Y*LKT	-1	-1	53	27
PY*LKT	0	-1	<10	17
Y*LKTK	2	-8	24	38
PYLKTK	100	111	>1mM	>1mM
PY*LKTK	3	-1	12	17
AY*LKTK	2	-1	18	35
AAPY*LKTK	0	1	25	16

Table 1. Affinity comparison of STAT3 phosphotyrosine-sequence derived peptides. The peptides were tested in the Flag-tag based STAT3 dimerization assay after preincubation of the peptides with monomeric STAT3. The percentage inhibition was calculated as: % inhibition=(signal in the presence of peptide - background)x100/(signal in the absence of peptide - background). This was only determined at the highest concentration tested (i.e. 1 mM). The IC_{50} was determined by nonlinear regression using the RS1 software.

5.2.3.2 Peptidomimetics

Substitution of the –1 position with benzyl-, pyridyl-, or pyrazinyl-derivatives, and in particular with a 4-cyanobenzoat, has been shown to increase the affinity of peptide PY*L Turkson *et al.* (2004). However, using the Flag-ELISA assay described here, no increase, but rather a decrease in affinity was measured in comparison to peptides PY*L or Y*L, when this position was substituted. This is in line with the observations made in the crystal structure, and the results obtained with the tested peptides (Table 1), which did not show an important contribution to binding by this position. The finding that the affinity of the peptidomimetics showed decreased values, could be due to the fact that (Turkson *et al.* 2004) tested them in the EMSA described before, which measures the capacity of compounds to disrupt preformed STAT3 dimers, while in this work the inhibition was measured in the Flag-ELISA, which measures binding to the SH2-domain directly.

	R'	% Control at 1mM	IC50 (µM)
Y*L	-	1	66
PY*L		0	68
ISS 593		9	184
ISS 249		100	>1mM
ISS 493		90	>200
ISS 353		60	>1mM
ISS 265		84	>1mM
ISS 610		6	180
ISS 637		100	>1mM
ISS 360		30	650

Table 2. Affinity comparison of peptidomimetics derived from STAT3-phospho-tyrosine-sequence. The structural formula of compounds: R'Y*L, where R' is defined as shown. The peptidomimetics were tested in the Flag-tag based STAT3 dimerization assay after preincubation with monomeric STAT3. The percentage inhibition was calculated by % control= (signal in the presence of peptide - background)x100/(signal in the absence of peptide - background). This was only determined at the highest concentration tested (i.e. 1 mM). The IC_{50} was determined by nonlinear regression using the RS1 software.

5.2.3.3 Small molecules

Docking of 5474 compounds of the Emmanuel Merck Darmstadt (EMD) compound pool onto the phosphotyrosine binding site of STAT3 using Virtual Ligand Screening (VLS) with FlexX and FLO+ programs resulted in the selection of 78 compounds (done by Ulrich Rester, Merck Darmstadt), which were tested in the STAT3 Flag-tag-based dimerization assay. All compounds were tested at 150 µM and in duplicates. The IC_{50} values were only determined for compounds that presented an inhibition higher than 40% at 150 µM. Out of the tested substances, 22 showed inhibition at 150 µM. From the chemical entities that could be validated by HPLC and mass spectroscopy, only one showed significant inhibition, with an IC_{50} value of around 15 µM (Fig. 39A).

STAT3 is predominantly dimerized in tumor cells, and it is therefore of interest to study the capacity of compounds to inhibit the activity of preformed dimers. Whole cell lysates of NIH3T3-TKS3 cells, which contain high amounts of activated STAT3, were preincubated with the dimerization inhibitor and tested for their capacity to bind DNA. The compound showed inhibition also under these conditions, in this case with an IC_{50} of 245 µM (Fig. 39B).

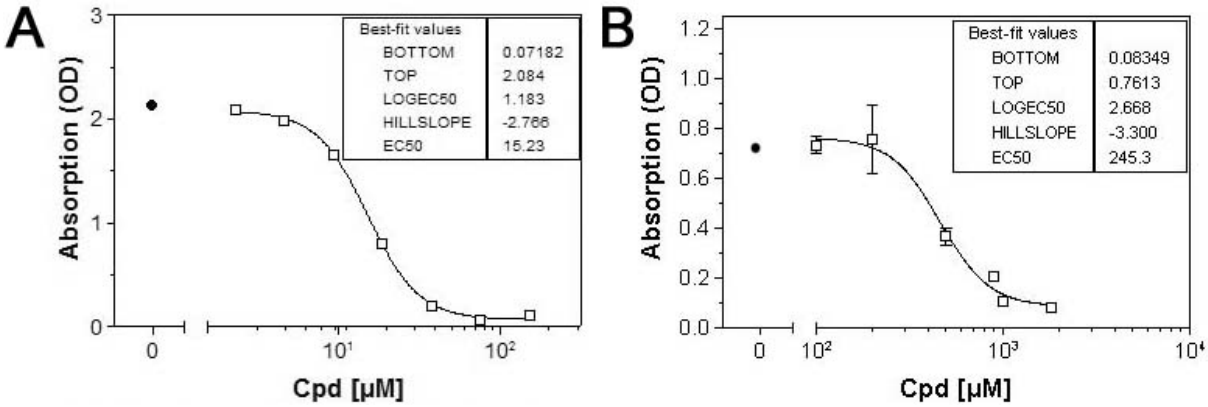

Fig.41. Compound 1 has an IC_{50} of 15 µM for dimerization inhibition, and an IC_{50} of 245 µM for disruption of dimerization. Compound 1 was dissolved in DMSO, preincubated for 30 min A) with STAT3-containing Sf9 cell lysates, and tested in the Flag-tag based ELISA, or B) with NIH3T3-TKS3 nuclear extracts, and tested in the DNA-binding ELISA. Black dots indicate the values obtained with the DMSO control.

6 DISCUSSION

6.1 Role of STAT3 in transformation of human cells

6.1.1 STAT3 oncogenic function in human cells

Activation of STAT3 has been observed in a broad variety of human tumors. It is constitutively activated in approximately 80% of human breast tumors, 70% of prostate cancers, 70% of ovarian cancers, 70% of nasopharingeal carcinomas, and in many head and neck cancers (Garcia *et al.* 2001;Savarese *et al.* 2002;Huang *et al.* 2000;Hsiao *et al.* 2003;Song and Grandis 2000). Additionally, it has been shown that STAT3 is involved in the transformation by different oncogenes, such as soluble tyrosine kinases like Src or the nucleophosmin-anaplastic lymphoma kinase (NPM-ALK) (Garcia *et al.* 1997;Cao *et al.* 1996;Zamo *et al.* 2002), and epidermal growth factor receptor family members, such as ErbB2 (Fernandes *et al.* 1999). Furthermore, the fact that STAT3 induces genes such as cyclin D1, c-myc, and bcl-xl, which promote growth and inhibit apoptosis, indicates a direct role for this transcription factor in cancer development. Different studies have further shown an essential role played by STAT3 in the transformation by many of these oncogenes (Bromberg *et al.* 1998;Turkson *et al.* 1998;Amin *et al.* 2004;Rubin *et al.* 2000). Furthermore, *in vivo* inhibition of STAT3 in tumor xenografts of human squamous cell cancers of the head and neck (SCCHN) induces apoptosis in the tumor tissue (Grandis *et al.* 2000). Altogether, these studies suggest that STAT3 activation is essential for human tumor development. In the mouse, *in vivo* inhibition of STAT3 in melanomas has also been reported to induce tumor regression (Niu *et al.* 1999). Furthermore, it has been shown that fibroblasts (NIH3T3 cells) can be transformed by a constitutively activated artificial mutant of STAT3 (STAT3C), and NIH3T3-STAT3C cells produce tumors in nude mice (Bromberg *et al.* 1999). However, the transforming capacity of activated STAT3 has not been shown in human cells.

In the present work, MCF10A cells were selected as a model system to study the transforming potency of active STAT3. This cell line is immortalized, but considered as not transformed, and it is commonly used to investigate molecular changes involved in the progression of human breast neoplasia. Full transformation of these

cells is difficult to achieve. For example, introduction of ErbB2 into these cells has been shown to induce preneoplastic properties, but not full transformation (Muthuswamy *et al.* 2001). Interestingly, it has been reported that c-Src is involved in the attachment independent growth of the MCFA-ErbB2 cells (Sheffield 1998). Since Src can directly phosphorylate STAT3, this kinase was chosen in this thesis to induce constitutive activation of STAT3 in MCF10A cells. In fact, MCF10A-v-Src cells showed persistent STAT3 phosphorylation, and, under growth factor deprivation, these cells showed increased proliferation and resistance to apoptosis. They also displayed anchorage independence, all of which indicated some degree of transformation. However, compared to NIH3T3-v-Src-TKS3 cells, which are NIH3T3 cells transformed by v-Src, and which also present constitutive STAT3 phosphorylation (Turkson *et al.* 1999), the oncogenic phenotype was less developed. NIH3T3-v-Src-TKS3 generated more and bigger colonies in soft agar than MCF10A-v-Src (Fig.6), and only NIH3T3-v-Src-TKS3 produced tumors in nude mice (Fig.12). It was somewhat surprising that MCF10A-v-Src cells were only weakly transformed, especially since v-Src is generally accepted as a strongly transforming oncogene (Frame 2004).

The different results observed in NIH3T3 and MCF10A cells might also reflect the fact that mouse cells can be transformed more easily than human cells, but it might also only be a specific property of these two cell lines. Many different reports show full transformation of NIH3T3 cells through introduction of diverse oncogenes, such as different viral oncogenes, Ras, AKT, c-kit, small GTPases, or fibroblast growth factor. However, the data available in the literature indicate that it seems to be more difficult to transform MCF10A cells. Various oncogenes have been studied in this cell line to test their tumorigenic capacity, but in fact only activated c-Ha-Ras has been shown to transform MCF10A cells sufficiently to induce tumor generation in nude mice (Wang *et al.* 1997). A number of the oncogenes studied in MCF10A cells induce only some of the typical properties of cancer cells, nonetheless these cells usually do not grow in soft agar, and should consequently not form tumors in nude mice. For example, studies using three-dimensional basement membrane cultures of MCF10A cells have shown that overexpression of cyclin D1 or inactivation of the retinoblastoma (Rb) protein by the introduction of human papillomavirus E7 in mammary epithelial acini results in excessive proliferation in the acinar structures, but it does not inhibit apoptosis, and hence does not transform the cells (Debnath *et al.*

2002). Furthermore, introduction of ErbB2 oncoprotein into MCF10A cells induces increased proliferation, protection from apoptosis, and changes in the apicobasal polarization of these cells. This results in the formation of multiacinar structures, which reflect a premalignant stage of breast cancer *in vivo*, the carcinoma in situ, but these cells retain their epithelial properties and do not form colonies in soft agar. These findings indicate that the ErbB2 transfected cells acquired a certain degree of preneoplastic changes, but not sufficient for full transformation (Muthuswamy *et al.* 2001).

Src introduction into MCF10A has not been reported yet, and the results of this thesis indicate that, similarly to ErbB2, this kinase can induce at least a preneoplastic transformation of these cells, which is reflected by their increased proliferation, resistance to apoptosis, and their anchorage independence (Fig.10 and 11). These cells acquired constitutive phosphorylation of STAT3 through the introduction of v-Src (Fig.9). Thus, the phenotypic changes observed in these cells might be due to STAT3 activity, but could also reflect v-Src-induced events that are not dependent on STAT3. It would be therefore interesting to study if STAT3 is essential for this preneoplastic transformation. Specific inhibition of STAT3 in these cells, using either DN-STAT3 or RNAi were attempted in the present work, but failed probably due to a poor transfection efficiency.

It should be expected that MCF10A-v-Src cells form multiacinar structures in three-dimensional basement membrane cultures like those obtained with ErbB2 transfected MCF10A cells. It would be of interest to know if coexpression of both Src and ErbB2 in MCF10A cells induced maximal activity of STAT3, for example through induction of its Ser-phosphorylation, known to be required for maximal activity of STAT3. This might enable the full transformation of these cells. Similar has been described for ErbB2 and TGFß, which have been reported to cooperate in the induction of migration and invasion (Seton-Rogers *et al.* 2004).

6.1.2 STAT3 inhibition for cancer treatment

Because STAT3 is often activated in many human cancers, inhibition of this molecule has been proposed to be a promising target for cancer treatment (Buettner *et al.* 2002). Inhibition of STAT3 activation has been shown to cause tumor regression in

two different tumor models: autologous mouse tumors grown in immunocompetent mice, and human tumor xenografts on athymic nude mice (Niu *et al.* 1999;Grandis *et al.* 2000). Niu et al. (1999) employed DN-STAT3 (STAT3β) injected directly into B16 murine melanomas by electroporation. The studies done by Grandis et al. (2000) were done with antisense STAT3.

The goal of this part of the present work was to generate a system in which one could specifically interfere with STAT3 signaling, to be used both in tissue culture and in human tumor xenografts. Hence, different inducible vectors expressing STAT3β were stably incorporated in tumor cells. DU145, a prostate cell line shown to be STAT3-dependent for survival (Mora *et al.* 2002), and which grows tumors in immunosuppressed mice, was chosen to study the effects of STAT3 inhibition *in vivo*. However, the levels of STAT3β induced in DU145 cells with the ecdysone system were shown to be very low, clearly under the levels of endogenous STAT3α (Fig.14), and no effects in proliferation or apoptosis could be measured upon expression of STAT3β (Fig.15).

Since STAT3β needs to heterodimerize with STAT3α to function as an inhibitor, this might explain the lack of effects observed in this study. STAT3β has to be present in stoichiometric majority in order to bind all STAT3α molecules, and inhibit STAT3 function completely. Using COS cells transfected with STAT3α and different amounts of the β isoform, it has been demonstrated that the transcriptional activity of STAT3α is partially inhibited using low amounts of STAT3β, but for complete inhibition, STAT3β needs to be transfected at higher levels than STAT3α, confirming that the wt molecule remains active in the case of insufficient expression of the DN (Caldenhoven *et al.* 1996).

Stronger expression was achieved using a tetracycline-inducible (Tet-On) system. In this case, even in full medium, 293-STAT3β cells treated with tetracycline showed a significant reduction of proliferation and induction of apoptosis. This is in line with the results reported by Rubin *et al.* (2000) and Buettner *et al.* (2002). Rubin *et al.* (2000)used SCCHN cells stably transfected with DN- or antisense STAT3 constructs, and studied apoptosis under starvation conditions. Buettner *et al.* (2002) showed that inhibition of STAT3 using antisense STAT3 oligonucleotides induced apoptosis in DU145 cells. In the present work it was also attempted to establish a STAT3β-inducible system in these cells, but stable introduction of the tetracycline repressor

(pcDNA6/TR), necessary to generate the Tet-On cell line, was not achieved. This was probably due to a poor transfection efficiency.

To control the effects observed in the established tetracycline-inducible system, knockdown of STAT3 was also attempted using STAT3 RNAi oligonucleotides. In human astrocytoma cells, introduction of STAT3 RNAi has been reported to induce apoptosis (Konnikova *et al.* 2003). In the current study, STAT3 RNAi did not decrease the levels of STAT3 in MCF10A-v-Src-B3 nor DU145 cells, most probably due a poor transfection rate, but it did so in 293. The 293 cells showed inhibition of proliferation and activation of apoptosis upon STAT3 RNAi treatment.

The inducible STAT3β expression system generated in this work provides an excellent tool to test the consequences of STAT3 inhibition on growth of developed human xenografts in nude mice: Induction of STAT3β through *in vivo* administration of doxycycline would lead to inhibtion of the hyperactivated STAT3, and thereby mimic pharmacological treatment with STAT3 inhibitors.

6.2 Rational design of STAT3 inhibitors

In the last decade, many drug discovery approaches have focused on targeting specific signal transduction pathways. In fact, small molecule inhibitors of receptor tyrosine kinases, farnesyltransferase, Raf and MEK are currently in clinical trials. Some inhibitors, such as the monoclonal antibodies against EGFR (cetuximab), and a small molecule inhibitor of the Bcr-Abl tyrosine kinase (STI-571), have already been approved for the treatment of certain tumors. No specific inhibitors of STAT3 with drug-like characteristics have been described so far.

The current knowledge of STAT3 allows envisioning different strategies to disrupt STAT3 activity: inhibition of the receptor ligand complexes or the kinases involved in STAT3 activation, or direct targeting of STAT3. For example, since STAT3 is constitutively activated by EGFR in HNSCC (Rubin *et al.* 2000), it can be expected that cetuximab could efficiently inhibit STAT3 phosphorylation and induce apoptosis in these cancers. Similarly, the EGFR specific compound ZD1839, and different tyrosine kinase inhibitors, such as the JAK blocker AG490, the Bcr-Abl inhibitor PD180970 and the Src inhibitor SU6656, can block the constitutive phosphorylation of STAT3, and inhibit the proliferation of diverse tumor cells (Li *et al.* 2003;Garcia *et al.* 2001;Laird *et al.* 2003). Furthermore, inhibition of STAT3 serine phosphorylation

with PD98059, a MAPK-pathway inhibitor, has been reported to block transformation induced by v-Src (Turkson *et al.* 1999).

The kinases that phosphorylate STAT3, such as Src, JAKs, EGFR, and PKC are known to affect many different pathways in the cell. Hence, one drawback of their inhibition would be the risk of unselective effects. However, STAT3 lies at the convergence point of different signaling pathways that stimulate growth-promoting genes, such as cyclin D1, c-myc, and bcl-xl, all of which play a role in tumor cell growth. Additionally, since STAT3 can be phosphorylated by many different kinases, to cover all different cells and tumors, many different receptor/ligand and kinase inhibitors would be required to inhibit STAT3 effectively. So, direct inhibition of STAT3 seems to be very promising for a highly selective treatment of many cancers.

A lot of information about the structure and activity of STAT3 has been published, importantly, its crystal structure (Becker *et al.* 1998). This enables a detailed analysis of the different domains, and allows a rational approach for the development of inhibitors.

6.2.1 Target site selection

The crystal structure of STAT3 was studied in the present work, and a precise pharmacophore was selected prior to screening compounds. Based on the function and on the physicochemical properties of different domains of STAT3, the SH2-domain was selected as the most promising target site. SH2-domains are modules of ~100 amino acids that bind to specific phosphotyrosine-containing peptide motifs. Compared to the DNA-binding domain, which also plays an essential role for the function of STATs and could therefore be another potential target site, the SH2-domain has a more moderate polarity and a more profound pocket. Both features are favorable for the design of small molecule inhibitors for intracellular targets.

In order to confirm the importance of the SH2-domain for the function of STAT3, peptides designed to block this site were tested and shown to disrupt STAT3 activation, which validated the selection of the SH2-domain as a good target site (Fig.26). This result was also observed by others, using similar phosphotyrosine peptides (Turkson *et al.* 2001). These experiments served as proof of principle for the selection of this site.

6.2.2 The similarity between STAT1 and STAT3 could hamper the selectivity of potential drugs

All STAT family members share a very similar structure, and some of them can form heterodimers, which indicates that their phosphotyrosine containing sequences and SH2-domains are very much alike. STAT3 can heterodimerize with STAT1. This explains why the STAT3-based peptides also inhibited STAT1 (Fig.26), however it is an undesirable feature, since STAT1 is considered to be a growth suppressor rather than a molecule involved in tumor development (Levy and Darnell, Jr. 2002).

By sequence comparison it has been shown in this work that within the STAT family, STAT1 shows the highest sequence homology in the SH2-domain, with 59% homology to STAT3 (Fig.27). However, the comparison of STAT1 and STAT3 SH2-domains in the crystal structures revealed structural differences that could be exploited to design specific STAT3 inhibitors (Fig.28 and 34). Furthermore, some conserved, but also some different interactions were identified at the phosphotyrosine-binding site in STAT1 and STAT3 dimers (Fig.31).

In the present work the characteristics of STAT SH2-domains were compared with SH2-domains of other crystallized proteins. At a sequence level, the SH2-domains of STATs are quite divergent from other SH2-containing proteins (Fig.27 and 33). However, the mechanism for recognizing the phosphotyrosine sequence is fundamentally the same as that for other SH2-domains (Kuriyan and Cowburn 1997): an antiparallel β sheet flanked by two α helices forms the core of the domain, and phosphorylated peptides bind perpendicular to the direction of the strands of the sheet (Fig.30A).

Interestingly, while the overall homology between Src and STAT3 SH2-domain is very low, they share around 40% homology at the core of the phosphotyrosine-interacting region, along a sequence of around 35 residues, starting at residue 582 of STAT3 (Fig.29). Two different pockets have been described for the binding of phosphotyrosine binding peptides on Src SH2-domain: one positively charged at the phosphotyrosine binding site, and a hydrophobic pocket that binds amino acid + 3 (Sawyer *et al.* 2001). By superimposition of the Src and STAT crystal structures it was found that the phosphotyrosine-binding site was highly conserved in all the structures, but not the hydrophobic pocket. The highly conserved Arg residue, which is conserved in all known SH2-domains, and which coordinates the phosphate

oxygens, superimposed very well in all the studied structures. In the present study, all the superimposed structures had three conserved phosphotyrosine binding partners (Arg^{609}, Ser^{611}, and Ser^{613} for STAT3). However, more variable residues contributed to specific recognition of residues that are C-terminal of the phosphotyrosine in STAT1 and STAT3 (Fig.30B and 31). Altogether, these results indicated that in order to design STAT3 specific inhibitors, not only the phosphotyrosine-binding site needed to be included in the target site, but also the pocket C-terminal of this site. STAT3 and Src SH2-domains differ sufficiently to allow for STAT3 inhibitors that should not bind to Src. However, the high structural similarity between STAT3 and STAT1 in this region might be an issue in terms of selectivity of potential inhibitors.

6.2.3 Assay development

Although the crystal structure provides important information that can help for the design of drugs, it is very important to validate in assays the observations made and the predictions deduced from the structure. Such assays need to allow for medium-throughput, and need to be sensitive enough to detect a high range of potencies of inhibitors. The assay established in the present work measured STAT3 dimerization, and showed to be specific, robust, stable and highly sensitive.

6.2.4 *In vitro* validation of structural predictions

The importance of specific residues in the SH2-domain for phosphopeptide binding was deduced from STAT3 dimeric crystal structure, which comprises the interaction of the phosphotyrosine sequence with the SH2-domain (Becker *et al.* 1998). The analysis revealed that residues - 1 to - 3 N-terminal of the phosphotyrosine (Ala^{702}, Ala^{703} and Pro^{704}), do not undergo any direct interactions with the SH2-domain, they rather protrude out of the interaction site. However, the residues C-terminal of the phosphotyrosine contribute to binding, especially the first three, which undergo close interactions with the SH2-domain, and also amino acid + 5. The side chains at positions + 1 (Leu^{706}), + 3 (Thr^{708}), and + 5 (Phe^{710}) penetrate into the SH2-domain, while those of positions + 2 and + 4 stick out of the binding site. Leu^{706} binds to a

pocket formed by Trp^{623}, Gln^{635}, Ser^{636}, Val^{637}, and Gln^{638}; Thr^{708} to Val^{637} and Tyr^{640}; and Phe^{710} to Tyr^{640} and Asn^{647} (Fig.31).

All published data (Turkson *et al.* 2001), and the results presented here point to a critical role of position + 1. Importantly, in the present work it was found that the minimal sequence showing inhibition in the dimerization assay was Y*L, further confirming the importance of Leu^{706} for binding to STAT3 SH2-domain.

The role of position –1 is less clear. Based on experimental testing of different phosphotyrosine peptides, Turkson *et al.* (2001) deduced an essential role for interactions at position –1. However, in the present work no specific interaction could be found at this site in the crystal structure, and no major difference in affinity was observed when this position was omitted in the peptides. Furthermore, peptide, PY* did not show inhibition, whereas different peptides lacking the Pro^{704} did. Nonetheless, it was observed that peptides that had Pro^{704} had a slightly increased affinity, as compared to peptides of the same length without the Pro^{704} (Table 1).

The difference between the role of Pro^{704} deduced from the crystal structure versus the results obtained with the peptides might reflect that the binding of the phosphotyrosine containing sequence is restricted in the dimer, because it is part of a long protein chain that could be constraining the conformations at this site, while peptides can bind more freely.

Addition of Ala^{702} and Ala^{703} to peptide PY*LKTK did not increase affinity, which was in accordance with the observations made in the crystal structure. In this case, possible structural constraints imposed by the protein chain did not seem to apply.

Based on the assumption that position - 1 was important, Turkson et al. (2004) developed peptidomimetics through substitution of Pro^{704} by benzyl-, pyridyl-, or pyrazinyl-derivatives. In particular, this group found that a 4-cyanobenzoat had increased affinity compared to peptide PY*L. However, using the Flag-ELISA assay these results could not be reproduced. Some of the peptidomimetics tested here showed inhibition of STAT3 dimerization, and among them, the 4-cyanobenzoat substitute showed the best affinity, as it did in the published work. However, compared to peptides PY*L or Y*L the binding was almost three times less potent in the dimerization assay (Table 2). This is in line with the observations made in the crystal structure, and with the results obtained with the tested peptides (Table 1), which did not show an important contribution to binding by this position.

The fact that the experiments made by Turkson et al. (2004) were made using EMSA, which measures the DNA-binding, but not directly the dimerization of STAT3, could be of relevance. The effects on DNA-binding require that the peptides disrupt preformed STAT3 dimers, which is different from blocking directly the free SH2-domain. The dimerization assay performed in the present work measures more directly the binding to the SH2-domain, which should account for more precise results. Molecules that inhibit the SH2-domain weakly might only be detected in the dimerization assay; however, potent SH2-inhibitors should also be able to disrupt preformed dimers.

The work presented here indicated that Thr^{708} and Phe^{710} were undergoing close interactions with the SH2-domain, although these were clearly not as important as the interaction at Leu^{706}. The results obtained with the Ala mutants confirmed that positions + 3 (Thr^{708}) contributes to binding, but less significantly than Leu^{706} (Table 1).

Not all the C-teminal residues of the phosphotyrosine undergo important interactions. In our studies, substitution of position + 2 with Ala did not prompt any decrease in the affinity, which is consistent with the observation that this amino acid interacts only with its backbone. In a recently published high-affinity peptide, position + 2 is occupied by a Pro^{704} (Ren *et al.* 2003). This group tested many substitutions for Lys^{707} but did not include an Ala. According to the observation made here, it should be expected that substitution of the Pro by an Ala in Y*LPQTV should not decrease the affinity of this peptide. However, position + 5 might have a more important role. The fact that the high-affinity peptide has an appropriate length to bind up to the binding site for Phe^{710} (Ren *et al.* 2003) is in accordance with the interactions observed at the binding site for Phe^{710} (i.e Tyr^{640} and Asn^{647}), indicating that the SH2-domain contains pockets in this region that can be used to optimize binding of compounds.

The peptides tested by Ren *et al.* (2003) included one phosphotyrosine peptide derived from STAT3 phosphotyrosine sequence, and the others were derived from the recruitment site for STAT3 at gp130. Studying the phosphotyrosine sequences of different cytokine receptors it has been reported that the pTyr-X-X-Gln is essential for STAT3 recruitment to the membrane (Stahl *et al.* 1995). Interestingly, the high-affinity peptide reported by Ren *et al.* (2003) has a Gln instead of a Thr^{708} at position + 3. It would therefore be expected that this amino acid maximizes the interactions at the

pocket that binds to the side chains of Thr^{708}. However, the side chain of Gln^{+3} does not seem to be appropriate to bind to the residues in the disposition they show in the crystal structure (Ren *et al.* 2003). Although the study of the crystal structure allowed to made predictions that are consistent with the experimental data obtained with the peptides, it is important to keep in mind that proteins are dynamic structures, and that crystal structures only provide a static view of their conformation. It might be that the SH2-domain can bind Gln^{+3} in the peptide through induced fitting by displacing some of the amino acids.

6.2.5 Virtual ligand screening (VLS) of small molecule inhibitors

Although high-throughput screening (HTS) is useful to find novel leads, screening of compound libraries by VLS is a promising alternative, when the structure of the protein is available. Structure-based drug design has already contributed to the discovery of a number of drugs that are presently in the market, among which some inhibitors of HIV-protease (nelfinavir, saquinavir, ritonavir, indinavir, amprenavir, and lopinavir), neuraminidase (zanamivir, oseltamivir), and carbonic anhydrase II (dorzolamide).

The structural analysis and the results obtained with the peptides and peptidomimetics encouraged the selection of the binding sites for Tyr^{705} through Thr^{708}. In the last decade, a lot of effort has been done to find SH2-inhibitors. Peptidomimetic and nonpeptide SH2-inhibitors of Src, Lck, Grb2, PI3-Kinase and Zap70 have been identified, which are active *in vivo* (Sawyer *et al.* 2002). Since it was found in the present work that the phosphotyrosine-binding site of STAT3 and Src is very similar, structures that have been successful in mimicking the phosphotyrosine were included in the compound pool. 5474 compounds were screened by the VLS, out of which 78 were tested in the dimerization assay. Out of these, one compound showed to inhibit dimerization with an IC_{50} of 15 µM, and was also able to disrupt preformed dimers. This is the first non-peptidic small molecule inhibitor of STAT3 identified so far, and might serve to study structure activity relationships (SAR) to optimize the structure and find more potent and bioavailable compounds.

7 REFERENCES

Akira, S. (2000). Roles of STAT3 defined by tissue-specific gene targeting. *Oncogene* **19**, 2607-2611.

Alberts, B., Bray, D., Lewis, M., Raff, M., Roberts, K., and Watson, J. D. Molecular Biology of the cell. 2002. Garland Publishing, Inc., New York, London.
Ref Type: Generic

Altschul, S. F., Bundschuh, R., Olsen, R., and Hwa, T. (2001). The estimation of statistical parameters for local alignment score distributions. *Nucleic Acids Res.* **29**, 351-361.

Amin, H. M., McDonnell, T. J., Ma, Y., Lin, Q., Fujio, Y., Kunisada, K., Leventaki, V., Das, P., Rassidakis, G. Z., Cutler, C., Jeffrey, Medeiros L., and Lai, R. (2004). Selective inhibition of STAT3 induces apoptosis and G(1) cell cycle arrest in ALK-positive anaplastic large cell lymphoma. *Oncogene*.

Atreya, R., Mudter, J., Finotto, S., Mullberg, J., Jostock, T., Wirtz, S., Schutz, M., Bartsch, B., Holtmann, M., Becker, C., Strand, D., Czaja, J., Schlaak, J. F., Lehr, H. A., Autschbach, F., Schurmann, G., Nishimoto, N., Yoshizaki, K., Ito, H., Kishimoto, T., Galle, P. R., Rose-John, S., and Neurath, M. F. (2000). Blockade of interleukin 6 trans signaling suppresses T-cell resistance against apoptosis in chronic intestinal inflammation: evidence in crohn disease and experimental colitis in vivo. *Nat.Med.* **6**, 583-588.

Barton, B. E., Karras, J. G., Murphy, T. F., Barton, A., and Huang, H. F. (2004). Signal transducer and activator of transcription 3 (STAT3) activation in prostate cancer: Direct STAT3 inhibition induces apoptosis in prostate cancer lines. *Mol.Cancer Ther.* **3**, 11-20.

Becker, S., Groner, B., and Muller, C. W. (1998). Three-dimensional structure of the Stat3beta homodimer bound to DNA. *Nature* **394**, 145-151.

Benekli, M., Xia, Z., Donohue, K. A., Ford, L. A., Pixley, L. A., Baer, M. R., Baumann, H., and Wetzler, M. (2002). Constitutive activity of signal transducer and activator of transcription 3 protein in acute myeloid leukemia blasts is associated with short disease-free survival. *Blood* **99**, 252-257.

Berclaz, G., Altermatt, H. J., Rohrbach, V., Siragusa, A., Dreher, E., and Smith, P. D. (2001). EGFR dependent expression of STAT3 (but not STAT1) in breast cancer. *Int.J.Oncol.* **19**, 1155-1160.

Boulton, T. G., Zhong, Z., Wen, Z., Darnell, J. E., Jr., Stahl, N., and Yancopoulos, G. D. (1995). STAT3 activation by cytokines utilizing gp130 and related transducers involves a secondary modification requiring an H7-sensitive kinase. *Proc.Natl.Acad.Sci.U.S.A* **92**, 6915-6919.

Braunstein, J., Brutsaert, S., Olson, R., and Schindler, C. (2003). STATs dimerize in the absence of phosphorylation. *J.Biol.Chem.* **278**, 34133-34140.

Bromberg, J. and Darnell, J. E., Jr. (2000). The role of STATs in transcriptional control and their impact on cellular function. *Oncogene* **19**, 2468-2473.

Bromberg, J. F., Horvath, C. M., Besser, D., Lathem, W. W., and Darnell, J. E., Jr. (1998). Stat3 activation is required for cellular transformation by v-src. *Mol.Cell Biol.* **18**, 2553-2558.

Bromberg, J. F., Wrzeszczynska, M. H., Devgan, G., Zhao, Y., Pestell, R. G., Albanese, C., and Darnell, J.-E. Jr (1999). Stat3 as an oncogene. *Cell* **98**, 295-303.

Buchholz, F., Angrand, P. O., and Stewart, A. F. (1996). A simple assay to determine the functionality of Cre or FLP recombination targets in genomic manipulation constructs. *Nucleic Acids Res.* **24**, 3118-3119.

Buettner, R., Mora, L. B., and Jove, R. (2002). Activated STAT signaling in human tumors provides novel molecular targets for therapeutic intervention
2. *Clin.Cancer Res.* **8**, 945-954.

Burke, W. M., Jin, X., Lin, H. J., Huang, M., Liu, R., Reynolds, R. K., and Lin, J. (2001). Inhibition of constitutively active Stat3 suppresses growth of human ovarian and breast cancer cells
9. *Oncogene* **20**, 7925-7934.

Caldenhoven, E., van Dijk, T. B., Solari, R., Armstrong, J., Raaijmakers, J. A., Lammers, J. W., Koenderman, L., and de Groot, R. P. (1996). STAT3beta, a splice variant of transcription factor STAT3, is a dominant negative regulator of transcription. *J.Biol.Chem.* **271**, 13221-13227.

Calo, V., Migliavacca, M., Bazan, V., Macaluso, M., Buscemi, M., Gebbia, N., and Russo, A. (2003). STAT proteins: from normal control of cellular events to tumorigenesis. *J.Cell Physiol* **197**, 157-168.

Campbell, C. L., Jiang, Z., Savarese, D. M., and Savarese, T. M. (2001). Increased expression of the interleukin-11 receptor and evidence of STAT3 activation in prostate carcinoma. *Am.J.Pathol.* **158**, 25-32.

Campbell, G. S., Yu, C. L., Jove, R., and Carter-Su, C. (1997). Constitutive activation of JAK1 in Src-transformed cells. *J.Biol.Chem.* **272**, 2591-2594.

Cantley, L. C. and Songyang, Z. (1994). Specificity in recognition of phosphopeptides by src-homology 2 domains. *J.Cell Sci.Suppl* **18**, 121-126.

Cao, X., Tay, A., Guy, G. R., and Tan, Y. H. (1996). Activation and association of Stat3 with Src in v-Src-transformed cell lines. *Mol.Cell Biol.* **16**, 1595-1603.

Ceresa, B. P., Horvath, C. M., and Pessin, J. E. (1997). Signal transducer and activator of transcription-3 serine phosphorylation by insulin is mediated by a Ras/Raf/MEK-dependent pathway. *Endocrinology* **138**, 4131-4137.

Chang, T. L., Mosoian, A., Pine, R., Klotman, M. E., and Moore, J. P. (2002). A soluble factor(s) secreted from CD8(+) T lymphocytes inhibits human immunodeficiency virus type 1 replication through STAT1 activation. *J.Virol.* **76**, 569-581.

Chen, X., Vinkemeier, U., Zhao, Y., Jeruzalmi, D., Darnell, J. E., Jr., and Kuriyan, J. (1998). Crystal structure of a tyrosine phosphorylated STAT-1 dimer bound to DNA. *Cell* **93**, 827-839.

Cheng, F., Wang, H. W., Cuenca, A., Huang, M., Ghansah, T., Brayer, J., Kerr, W. G., Takeda, K., Akira, S., Schoenberger, S. P., Yu, H., Jove, R., and Sotomayor, E. M. (2003). A critical role for Stat3 signaling in immune tolerance. *Immunity.* **19**, 425-436.

Chung, J., Uchida, E., Grammer, T. C., and Blenis, J. (1997). STAT3 serine phosphorylation by ERK-dependent and -independent pathways negatively modulates its tyrosine phosphorylation. *Mol.Cell Biol.* **17**, 6508-6516.

Church, D., Zhang, Y., Rago, R., and Wilding, G. (1999). Efficacy of suramin against human prostate carcinoma DU145 xenografts in nude mice. *Cancer Chemother.Pharmacol.* **43**, 198-204.

Coppo, P., Dusanter-Fourt, I., Millot, G., Nogueira, M. M., Dugray, A., Bonnet, M. L., Mitjavila-Garcia, M. T., Le Pesteur, D., Guilhot, F., Vainchenker, W., Sainteny, F., and Turhan, A. G. (2003). Constitutive and specific activation of STAT3 by BCR-ABL in embryonic stem cells. *Oncogene* **22**, 4102-4110.

Darnell, J. E., Jr. (2002). Transcription factors as targets for cancer therapy
20. *Nat.Rev.Cancer* **2**, 740-749.

David, M., Petricoin, E., III, Benjamin, C., Pine, R., Weber, M. J., and Larner, A. C. (1995). Requirement for MAP kinase (ERK2) activity in interferon alpha- and interferon beta-stimulated gene expression through STAT proteins. *Science* **269**, 1721-1723.

Debnath, J., Mills, K. R., Collins, N. L., Reginato, M. J., Muthuswamy, S. K., and Brugge, J. S. (2002). The role of apoptosis in creating and maintaining luminal space within normal and oncogene-expressing mammary acini. *Cell* **111**, 29-40.

Dhir, R., Ni, Z., Lou, W., DeMiguel, F., Grandis, J. R., and Gao, A. C. (2002). Stat3 activation in prostatic carcinomas
11. *Prostate* **51**, 241-246.

Dong, S., Chen, S. J., and Tweardy, D. J. (2003). Cross-talk between retinoic acid and STAT3 signaling pathways in acute promyelocytic leukemia. *Leuk.Lymphoma* **44**, 2023-2029.

Dunican, D. J. and Doherty, P. (2001). Designing cell-permeant phosphopeptides to modulate intracellular signaling pathways. *Biopolymers* **60**, 45-60.

Durbin, J. E., Hackenmiller, R., Simon, M. C., and Levy, D. E. (1996). Targeted disruption of the mouse Stat1 gene results in compromised innate immunity to viral disease. *Cell* **84**, 443-450.

Fagerlund, R., Melen, K., Kinnunen, L., and Julkunen, I. (2002). Arginine/lysine-rich nuclear localization signals mediate interactions between dimeric STATs and importin alpha 5. *J.Biol.Chem.* **277**, 30072-30078.

Fernandes, A., Hamburger, A. W., and Gerwin, B. I. (1999). ErbB-2 kinase is required for constitutive stat 3 activation in malignant human lung epithelial cells. *Int.J.Cancer* **83**, 564-570.

Frame, M. C. (2004). Newest findings on the oldest oncogene; how activated src does it
18. *J.Cell Sci.* **117**, 989-998.

Franks, L. M. and Teich, N. M. Introduction to the Cellular adn Molecular Biology of Cancer. 1997. University Press, Oxford, New York, Tokyo.
Ref Type: Generic

Fukada, T., Hibi, M., Yamanaka, Y., Takahashi-Tezuka, M., Fujitani, Y., Yamaguchi, T., Nakajima, K., and Hirano, T. (1996). Two signals are necessary for cell proliferation induced by a cytokine receptor gp130: involvement of STAT3 in anti-apoptosis. *Immunity.* **5**, 449-460.

Galm, O., Yoshikawa, H., Esteller, M., Osieka, R., and Herman, J. G. (2003). SOCS-1, a negative regulator of cytokine signaling, is frequently silenced by methylation in multiple myeloma. *Blood* **101**, 2784-2788.

Gao, B., Shen, X., Kunos, G., Meng, Q., Goldberg, I. D., Rosen, E. M., and Fan, S. (2001). Constitutive activation of JAK-STAT3 signaling by BRCA1 in human prostate cancer cells. *FEBS Lett.* **488**, 179-184.

Garcia, R., Bowman, T. L., Niu, G., Yu, H., Minton, S., Muro-Cacho, C. A., Cox, C. E., Falcone, R., Fairclough, R., Parsons, S., Laudano, A., Gazit, A., Levitzki, A., Kraker, A., and Jove, R. (2001). Constitutive activation of Stat3 by the Src and JAK tyrosine kinases participates in growth regulation of human breast carcinoma cells. *Oncogene* **20**, 2499-2513.

Garcia, R., Yu, C. L., Hudnall, A., Catlett, R., Nelson, K. L., Smithgall, T., Fujita, D. J., Ethier, S. P., and Jove, R. (1997). Constitutive activation of Stat3 in fibroblasts transformed by diverse oncoproteins and in breast carcinoma cells. *Cell Growth Differ.* **8**, 1267-1276.

Gollob, J. A., Schnipper, C. P., Murphy, E. A., Ritz, J., and Frank, D. A. (1999). The functional synergy between IL-12 and IL-2 involves p38 mitogen-activated protein kinase and is associated with the augmentation of STAT serine phosphorylation. *J.Immunol.* **162**, 4472-4481.

Gonzalez, F. A., Raden, D. L., and Davis, R. J. (1991). Identification of substrate recognition determinants for human ERK1 and ERK2 protein kinases. *J.Biol.Chem.* **266**, 22159-22163.

Gouilleux-Gruart, V., Debierre-Grockiego, F., Gouilleux, F., Capiod, J. C., Claisse, J. F., Delobel, J., and Prin, L. (1997). Activated Stat related transcription factors in acute leukemia. *Leuk.Lymphoma* **28**, 83-88.

Graham, F. L. (1987). Growth of 293 cells in suspension culture. *J.Gen.Virol.* **68 (Pt 3)**, 937-940.

Grandis, J. R., Drenning, S. D., Zeng, Q., Watkins, S. C., Melhem, M. F., Endo, S., Johnson, D. E., Huang, L., He, Y., and Kim, J. D. (2000). Constitutive activation of Stat3 signaling abrogates apoptosis in squamous cell carcinogenesis in vivo. *Proc.Natl.Acad.Sci.U.S.A* **97**, 4227-4232.

Guan, L. S., Li, G. C., Chen, C. C., Liu, L. Q., and Wang, Z. Y. (2001). Rb-associated protein 46 (RbAp46) suppresses the tumorigenicity of adenovirus-transformed human embryonic kidney 293 cells. *Int.J.Cancer* **93**, 333-338.

Haan, S., Hemmann, U., Hassiepen, U., Schaper, F., Schneider-Mergener, J., Wollmer, A., Heinrich, P. C., and Grotzinger, J. (1999). Characterization and binding specificity of the monomeric STAT3-SH2 domain. *J.Biol.Chem.* **274**, 1342-1348.

Haan, S., Kortylewski, M., Behrmann, I., Muller-Esterl, W., Heinrich, P. C., and Schaper, F. (2000). Cytoplasmic STAT proteins associate prior to activation. *Biochem.J.* **345 Pt 3**, 417-421.

Horiguchi, A., Oya, M., Shimada, T., Uchida, A., Marumo, K., and Murai, M. (2002). Activation of signal transducer and activator of transcription 3 in renal cell carcinoma: a study of incidence and its association with pathological features and clinical outcome
7. *J.Urol.* **168**, 762-765.

Horvath, C. M., Wen, Z., and Darnell, J. E., Jr. (1995). A STAT protein domain that determines DNA sequence recognition suggests a novel DNA-binding domain. *Genes Dev.* **9**, 984-994.

Hsiao, J. R., Jin, Y. T., Tsai, S. T., Shiau, A. L., Wu, C. L., and Su, W. C. (2003). Constitutive activation of STAT3 and STAT5 is present in the majority of nasopharyngeal carcinoma and correlates with better prognosis. *Br.J.Cancer* **89**, 344-349.

Huang, D. C., Cory, S., and Strasser, A. (1997). Bcl-2, Bcl-XL and adenovirus protein E1B19kD are functionally equivalent in their ability to inhibit cell death. *Oncogene* **14**, 405-414.

Huang, M., Page, C., Reynolds, R. K., and Lin, J. (2000). Constitutive activation of stat 3 oncogene product in human ovarian carcinoma cells. *Gynecol.Oncol.* **79**, 67-73.

Improta, T. and Pine, R. (1997). Susceptibility to virus infection is determined by a Stat-mediated response to the autocrine effect of virus-induced type I interferon. *Cytokine* **9**, 383-393.

Jain, N., Zhang, T., Kee, W. H., Li, W., and Cao, X. (1999). Protein kinase C delta associates with and phosphorylates Stat3 in an interleukin-6-dependent manner. *J.Biol.Chem.* **274**, 24392-24400.

Johnson, P. J., Coussens, P. M., Danko, A. V., and Shalloway, D. (1985). Overexpressed pp60c-src can induce focus formation without complete transformation of NIH 3T3 cells. *Mol.Cell Biol.* **5**, 1073-1083.

Kaplan, M. H. and Grusby, M. J. (1998). Regulation of T helper cell differentiation by STAT molecules. *J.Leukoc.Biol.* **64**, 2-5.

Kaplan, M. H., Sun, Y. L., Hoey, T., and Grusby, M. J. (1996). Impaired IL-12 responses and enhanced development of Th2 cells in Stat4-deficient mice. *Nature* **382**, 174-177.

Kimura, T., Kadokawa, Y., Harada, H., Matsumoto, M., Sato, M., Kashiwazaki, Y., Tarutani, M., Tan, R. S., Takasugi, T., Matsuyama, T., Mak, T. W., Noguchi, S., and Taniguchi, T. (1996). Essential and non-redundant roles of p48 (ISGF3 gamma) and IRF-1 in both type I and type II interferon responses, as revealed by gene targeting studies. *Genes Cells* **1**, 115-124.

Kmiecik, T. E. and Shalloway, D. (1987). Activation and suppression of pp60c-src transforming ability by mutation of its primary sites of tyrosine phosphorylation. *Cell* **49**, 65-73.

Konnikova, L., Kotecki, M., Kruger, M. M., and Cochran, B. H. (2003). Knockdown of STAT3 expression by RNAi induces apoptosis in astrocytoma cells. *BMC.Cancer* **3**, 23.

Krause, A., Scaletta, N., Ji, J. D., and Ivashkiv, L. B. (2002). Rheumatoid arthritis synoviocyte survival is dependent on Stat3. *J.Immunol.* **169**, 6610-6616.

Kretzschmar, A. K., Dinger, M. C., Henze, C., Brocke-Heidrich, K., and Horn, F. (2004). Analysis of Stat3 (signal transducer and activator of transcription 3) dimerization by fluorescence resonance energy transfer in living cells. *Biochem.J.* **377**, 289-297.

Kube, D., Holtick, U., Vockerodt, M., Ahmadi, T., Haier, B., Behrmann, I., Heinrich, P. C., Diehl, V., and Tesch, H. (2001). STAT3 is constitutively activated in Hodgkin cell lines. *Blood* **98**, 762-770.

Kuo, C. T. and Leiden, J. M. (1999). Transcriptional regulation of T lymphocyte development and function. *Annu.Rev.Immunol.* **17**, 149-187.

Kuriyan, J. and Cowburn, D. (1997). Modular peptide recognition domains in eukaryotic signaling. *Annu.Rev.Biophys.Biomol.Struct.* **26**, 259-288.

Kuroki, M. and O'Flaherty, J. T. (1999). Extracellular signal-regulated protein kinase (ERK)-dependent and ERK-independent pathways target STAT3 on serine-727 in human neutrophils stimulated by chemotactic factors and cytokines. *Biochem.J.* **341 (Pt 3)**, 691-696.

Laird, A. D., Li, G., Moss, K. G., Blake, R. A., Broome, M. A., Cherrington, J. M., and Mendel, D. B. (2003). Src family kinase activity is required for signal tranducer and activator of transcription 3 and focal adhesion kinase phosphorylation and vascular endothelial growth factor signaling in vivo and for anchorage-dependent and -independent growth of human tumor cells. *Mol.Cancer Ther.* **2**, 461-469.

Lee, R. J., Albanese, C., Stenger, R. J., Watanabe, G., Inghirami, G., Haines, G. K., III, Webster, M., Muller, W. J., Brugge, J. S., Davis, R. J., and Pestell, R. G. (1999). pp60(v-src) induction of cyclin D1 requires collaborative interactions between the extracellular signal-regulated kinase, p38, and Jun kinase pathways. A role for cAMP response element-binding protein and activating transcription factor-2 in pp60(v-src) signaling in cancer cells. *J.Biol.Chem.* **274**, 7341-7350.

Levy, D. E. and Darnell, J. E., Jr. (2002). Stats: transcriptional control and biological impact. *Nat.Rev.Mol.Cell Biol.* **3**, 651-662.

Li, B., Chang, C. M., Yuan, M., McKenna, W. G., and Shu, H. K. (2003). Resistance to small molecule inhibitors of epidermal growth factor receptor in malignant gliomas. *Cancer Res.* **63**, 7443-7450.

Lim, C. P. and Cao, X. (1999). Serine phosphorylation and negative regulation of Stat3 by JNK. *J.Biol.Chem.* **274**, 31055-31061.

Lin, J., Jin, X., Rothman, K., Lin, H. J., Tang, H., and Burke, W. (2002). Modulation of signal transducer and activator of transcription 3 activities by p53 tumor suppressor in breast cancer cells. *Cancer Res.* **62**, 376-380.

Lin, T. S., Mahajan, S., and Frank, D. A. (2000). STAT signaling in the pathogenesis and treatment of leukemias
13. *Oncogene* **19**, 2496-2504.

Liu, H. and Pope, R. M. (2003). The role of apoptosis in rheumatoid arthritis. *Curr.Opin.Pharmacol.* **3**, 317-322.

Liu, X., Robinson, G. W., Wagner, K. U., Garrett, L., Wynshaw-Boris, A., and Hennighausen, L. (1997). Stat5a is mandatory for adult mammary gland development and lactogenesis. *Genes Dev.* **11**, 179-186.

Lodish, H., Baltimore, D., Berk, A., Zipursky, S., Matsudaira, P., and Darnell, J. Molecular cell biology. 2003. Scientific American Books, New York.
Ref Type: Generic

Lou, W., Ni, Z., Dyer, K., Tweardy, D. J., and Gao, A. C. (2000). Interleukin-6 induces prostate cancer cell growth accompanied by activation of stat3 signaling pathway. *Prostate* **42**, 239-242.

Lovato, P., Brender, C., Agnholt, J., Kelsen, J., Kaltoft, K., Svejgaard, A., Eriksen, K. W., Woetmann, A., and Odum, N. (2003). Constitutive STAT3 activation in intestinal T cells from patients with Crohn's disease. *J.Biol.Chem.* **278**, 16777-16781.

McBride, K. M., Banninger, G., McDonald, C., and Reich, N. C. (2002). Regulated nuclear import of the STAT1 transcription factor by direct binding of importin-alpha. *EMBO J.* **21**, 1754-1763.

McBride, K. M., McDonald, C., and Reich, N. C. (2000). Nuclear export signal located within theDNA-binding domain of the STAT1transcription factor. *EMBO J.* **19**, 6196-6206.

Melen, K., Kinnunen, L., and Julkunen, I. (2001). Arginine/lysine-rich structural element is involved in interferon-induced nuclear import of STATs. *J.Biol.Chem.* **276**, 16447-16455.

Meraz, M. A., White, J. M., Sheehan, K. C., Bach, E. A., Rodig, S. J., Dighe, A. S., Kaplan, D. H., Riley, J. K., Greenlund, A. C., Campbell, D., Carver-Moore, K., DuBois, R. N., Clark, R., Aguet, M., and Schreiber, R. D. (1996). Targeted disruption of the Stat1 gene in mice reveals unexpected physiologic specificity in the JAK-STAT signaling pathway. *Cell* **84**, 431-442.

Mikita, T., Campbell, D., Wu, P., Williamson, K., and Schindler, U. (1996). Requirements for interleukin-4-induced gene expression and functional characterization of Stat6. *Mol.Cell Biol.* **16**, 5811-5820.

Mohrs, M., Lacy, D. A., and Locksley, R. M. (2003). Stat signals release activated naive Th cells from an anergic checkpoint. *J.Immunol.* **170**, 1870-1876.

Mora, L. B., Buettner, R., Seigne, J., Diaz, J., Ahmad, N., Garcia, R., Bowman, T., Falcone, R., Fairclough, R., Cantor, A., Muro-Cacho, C., Livingston, S., Karras, J., Pow-Sang, J., and Jove, R. (2002). Constitutive activation of Stat3 in human prostate tumors and cell lines: direct inhibition of Stat3 signaling induces apoptosis of prostate cancer cells. *Cancer Res.* **62**, 6659-6666.

Moriggl, R., Topham, D. J., Teglund, S., Sexl, V., McKay, C., Wang, D., Hoffmeyer, A., van Deursen, J., Sangster, M. Y., Bunting, K. D., Grosveld, G. C., and Ihle, J. N. (1999). Stat5 is required for IL-2-induced cell cycle progression of peripheral T cells. *Immunity.* **10**, 249-259.

Muthuswamy, S. K., Li, D., Lelievre, S., Bissell, M. J., and Brugge, J. S. (2001). ErbB2, but not ErbB1, reinitiates proliferation and induces luminal repopulation in epithelial acini. *Nat.Cell Biol.* **3**, 785-792.

Ng, J. and Cantrell, D. (1997). STAT3 is a serine kinase target in T lymphocytes. Interleukin 2 and T cell antigen receptor signals converge upon serine 727. *J.Biol.Chem.* **272**, 24542-24549.

Niculescu, F. and Rus, H. (1999). Complement activation and atherosclerosis. *Mol.Immunol.* **36**, 949-955.

Ning, Z. Q., Li, J., McGuinness, M., and Arceci, R. J. (2001). STAT3 activation is required for Asp(816) mutant c-Kit induced tumorigenicity. *Oncogene* **20**, 4528-4536.

Niu, G., Bowman, T., Huang, M., Shivers, S., Reintgen, D., Daud, A., Chang, A., Kraker, A., Jove, R., and Yu, H. (2002). Roles of activated Src and Stat3 signaling in melanoma tumor cell growth. *Oncogene* **21**, 7001-7010.

Niu, G., Heller, R., Catlett-Falcone, R., Coppola, D., Jaroszeski, M., Dalton, W., Jove, R., and Yu, H. (1999). Gene therapy with dominant-negative Stat3 suppresses growth of the murine melanoma B16 tumor in vivo
4. *Cancer Res.* **59**, 5059-5063.

Niu, G., Shain, K. H., Huang, M., Ravi, R., Bedi, A., Dalton, W. S., Jove, R., and Yu, H. (2001). Overexpression of a dominant-negative signal transducer and activator of

transcription 3 variant in tumor cells leads to production of soluble factors that induce apoptosis and cell cycle arrest
3. *Cancer Res.* **61**, 3276-3280.

Onishi, M., Nosaka, T., Misawa, K., Mui, A. L., Gorman, D., McMahon, M., Miyajima, A., and Kitamura, T. (1998). Identification and characterization of a constitutively active STAT5 mutant that promotes cell proliferation. *Mol.Cell Biol.* **18**, 3871-3879.

Ostrand-Rosenberg, S., Sinha, P., Clements, V., Dissanayake, S. I., Miller, S., Davis, C., and Danna, E. (2004). Signal transducer and activator of transcription 6 (Stat6) and CD1: inhibitors of immunosurveillance against primary tumors and metastatic disease. *Cancer Immunol.Immunother.* **53**, 86-91.

Page, C., Huang, M., Jin, X., Cho, K., Lilja, J., Reynolds, R. K., and Lin, J. (2000). Elevated phosphorylation of AKT and Stat3 in prostate, , and cervical cancer cells. *Int.J.Oncol.* **17**, 23-28.

Raz, R., Durbin, J. E., and Levy, D. E. (1994). Acute phase response factor and additional members of the interferon-stimulated gene factor 3 family integrate diverse signals from cytokines, interferons, and growth factors. *J.Biol.Chem.* **269**, 24391-24395.

Ren, Z., Cabell, L. A., Schaefer, T. S., and McMurray, J. S. (2003). Identification of a high-affinity phosphopeptide inhibitor of Stat3. *Bioorg.Med.Chem.Lett.* **13**, 633-636.

Rubin, Grandis J., Zeng, Q., and Drenning, S. D. (2000). Epidermal growth factor receptor--mediated stat3 signaling blocks apoptosis in head and neck cancer
5. *Laryngoscope* **110**, 868-874.

Sano, S., Itami, S., Takeda, K., Tarutani, M., Yamaguchi, Y., Miura, H., Yoshikawa, K., Akira, S., and Takeda, J. (1999). Keratinocyte-specific ablation of Stat3 exhibits impaired skin remodeling, but does not affect skin morphogenesis. *EMBO J.* **18**, 4657-4668.

Savarese, T. M., Campbell, C. L., McQuain, C., Mitchell, K., Guardiani, R., Quesenberry, P. J., and Nelson, B. E. (2002). Coexpression of oncostatin M and its receptors and evidence for STAT3 activation in human ovarian carcinomas
8. *Cytokine* **17**, 324-334.

Sawyer, T., Boyce, B., Dalgarno, D., and Iuliucci, J. (2001). Src inhibitors: genomics to therapeutics. *Expert.Opin.Investig.Drugs* **10**, 1327-1344.

Sawyer, T. K., Bohacek, R. S., Dalgarno, D. C., Eyermann, C. J., Kawahata, N., Metcalf, C. A., III, Shakespeare, W. C., Sundaramoorthi, R., Wang, Y., and Yang, M. G. (2002). SRC homology-2 inhibitors: peptidomimetic and nonpeptide. *Mini.Rev.Med.Chem.* **2**, 475-488.

Schaeffer, H. J. and Weber, M. J. (1999). Mitogen-activated protein kinases: specific messages from ubiquitous messengers. *Mol.Cell Biol.* **19**, 2435-2444.

Schaffer, A. A., Aravind, L., Madden, T. L., Shavirin, S., Spouge, J. L., Wolf, Y. I., Koonin, E. V., and Altschul, S. F. (2001). Improving the accuracy of PSI-BLAST

protein database searches with composition-based statistics and other refinements. *Nucleic Acids Res.* **29**, 2994-3005.

Schindler, C. and Darnell, J. E., Jr. (1995). Transcriptional responses to polypeptide ligands: the JAK-STAT pathway. *Annu.Rev.Biochem.* **64**, 621-651.

Schindler, U., Wu, P., Rothe, M., Brasseur, M., and McKnight, S. L. (1995). Components of a Stat recognition code: evidence for two layers of molecular selectivity. *Immunity.* **2**, 689-697.

Schroder, M., Kroeger, K. M., Volk, H. D., Eidne, K. A., and Grutz, G. (2004). Preassociation of nonactivated STAT3 molecules demonstrated in living cells using bioluminescence resonance energy transfer: a new model of STAT activation? *J.Leukoc.Biol.* **75**, 792-797.

Schuringa, J. J., Wierenga, A. T., Kruijer, W., and Vellenga, E. (2000). Constitutive Stat3, Tyr705, and Ser727 phosphorylation in acute myeloid leukemia cells caused by the autocrine secretion of interleukin-6. *Blood* **95**, 3765-3770.

Seidel, H. M., Milocco, L. H., Lamb, P., Darnell, J. E., Jr., Stein, R. B., and Rosen, J. (1995). Spacing of palindromic half sites as a determinant of selective STAT (signal transducers and activators of transcription) DNA binding and transcriptional activity. *Proc.Natl.Acad.Sci.U.S.A* **92**, 3041-3045.

Seton-Rogers, S. E., Lu, Y., Hines, L. M., Koundinya, M., LaBaer, J., Muthuswamy, S. K., and Brugge, J. S. (2004). Cooperation of the ErbB2 receptor and transforming growth factor beta in induction of migration and invasion in mammary epithelial cells. *Proc.Natl.Acad.Sci.U.S.A* **101**, 1257-1262.

Sheffield, L. G. (1998). C-Src activation by ErbB2 leads to attachment-independent growth of human breast epithelial cells. *Biochem.Biophys.Res.Commun.* **250**, 27-31.

Shimoda, K., van Deursen, J., Sangster, M. Y., Sarawar, S. R., Carson, R. T., Tripp, R. A., Chu, C., Quelle, F. W., Nosaka, T., Vignali, D. A., Doherty, P. C., Grosveld, G., Paul, W. E., and Ihle, J. N. (1996). Lack of IL-4-induced Th2 response and IgE class switching in mice with disrupted Stat6 gene. *Nature* **380**, 630-633.

Shuai, K., Ziemiecki, A., Wilks, A. F., Harpur, A. G., Sadowski, H. B., Gilman, M. Z., and Darnell, J. E. (1993). Polypeptide signaling to the nucleus through tyrosine phosphorylation of JAK and Stat proteins
22. *Nature* **366**, 580-583.

Song, J. I. and Grandis, J. R. (2000). STAT signaling in head and neck cancer. *Oncogene* **19**, 2489-2495.

Soule, H. D., Maloney, T. M., Wolman, S. R., Peterson, W.-D. Jr, Brenz, R., McGrath, C. M., Russo, J., Pauley, R. J., Jones, R. F., and Brooks, S. C. (1990). Isolation and characterization of a spontaneously immortalized human epithelial cell line, MCF-10. *Cancer Res.* **50**, 6075-6086.

Spiekermann, K., Biethahn, S., Wilde, S., Hiddemann, W., and Alves, F. (2001). Constitutive activation of STAT transcription factors in acute myelogenous leukemia. *Eur.J.Haematol.* **67**, 63-71.

Stahl, N., Farruggella, T. J., Boulton, T. G., Zhong, Z., Darnell, J. E., Jr., and Yancopoulos, G. D. (1995). Choice of STATs and other substrates specified by modular tyrosine-based motifs in cytokine receptors. *Science* **267**, 1349-1353.

Stanbridge, E. J. and Perkins, F. T. (1976). Tumourigenicity testing in immunosuppressed mice: advantages and disadvantages. *Dev.Biol.Stand.* **37**, 211-217.

Stephanou, A. and Latchman, D. S. (2003). STAT-1: a novel regulator of apoptosis. *Int.J.Exp.Pathol.* **84**, 239-244.

Strehlow, I. and Schindler, C. (1998). Amino-terminal signal transducer and activator of transcription (STAT) domains regulate nuclear translocation and STAT deactivation. *J.Biol.Chem.* **273**, 28049-28056.

Summy, J. M. and Gallick, G. E. (2003). Src family kinases in tumor progression and metastasis. *Cancer Metastasis Rev.* **22**, 337-358.

Takeda, K., Kaisho, T., Yoshida, N., Takeda, J., Kishimoto, T., and Akira, S. (1998). Stat3 activation is responsible for IL-6-dependent T cell proliferation through preventing apoptosis: generation and characterization of T cell-specific Stat3-deficient mice. *J.Immunol.* **161**, 4652-4660.

Takeda, K., Noguchi, K., Shi, W., Tanaka, T., Matsumoto, M., Yoshida, N., Kishimoto, T., and Akira, S. (1997). Targeted disruption of the mouse Stat3 gene leads to early embryonic lethality. *Proc.Natl.Acad.Sci.U.S.A* **94**, 3801-3804.

Takeda, K., Tanaka, T., Shi, W., Matsumoto, M., Minami, M., Kashiwamura, S., Nakanishi, K., Yoshida, N., Kishimoto, T., and Akira, S. (1996). Essential role of Stat6 in IL-4 signaling. *Nature* **380**, 627-630.

Takemoto, S., Mulloy, J. C., Cereseto, A., Migone, T. S., Patel, B. K., Matsuoka, M., Yamaguchi, K., Takatsuki, K., Kamihira, S., White, J. D., Leonard, W. J., Waldmann, T., and Franchini, G. (1997). Proliferation of adult T cell leukemia/lymphoma cells is associated with the constitutive activation of JAK/STAT proteins. *Proc.Natl.Acad.Sci.U.S.A* **94**, 13897-13902.

Teglund, S., McKay, C., Schuetz, E., van Deursen, J. M., Stravopodis, D., Wang, D., Brown, M., Bodner, S., Grosveld, G., and Ihle, J. N. (1998). Stat5a and Stat5b proteins have essential and nonessential, or redundant, roles in cytokine responses. *Cell* **93**, 841-850.

Thierfelder, W. E., van Deursen, J. M., Yamamoto, K., Tripp, R. A., Sarawar, S. R., Carson, R. T., Sangster, M. Y., Vignali, D. A., Doherty, P. C., Grosveld, G. C., and Ihle, J. N. (1996). Requirement for Stat4 in interleukin-12-mediated responses of natural killer and T cells. *Nature* **382**, 171-174.

Towatari, M. and Iida, H. (1998). [Constitutive activation of MAP kinase pathway and STAT pathway in AML]. *Rinsho Ketsueki* **39**, 86-88.

Turkson, J., Bowman, T., Adnane, J., Zhang, Y., Djeu, J. Y., Sekharam, M., Frank, D. A., Holzman, L. B., Wu, J., Sebti, S., and Jove, R. (1999). Requirement for

Ras/Rac1-mediated p38 and c-Jun N-terminal kinase signaling in Stat3 transcriptional activity induced by the Src oncoprotein. *Mol.Cell Biol.* **19**, 7519-7528.

Turkson, J., Bowman, T., Garcia, R., Caldenhoven, E., de Groot, R. P., and Jove, R. (1998). Stat3 activation by Src induces specific gene regulation and is required for cell transformation. *Mol.Cell Biol.* **18**, 2545-2552.

Turkson, J., Kim, J. S., Zhang, S., Yuan, J., Huang, M., Glenn, M., Haura, E., Sebti, S., Hamilton, A. D., and Jove, R. (2004). Novel peptidomimetic inhibitors of signal transducer and activator of transcription 3 dimerization and biological activity. *Mol.Cancer Ther.* **3**, 261-269.

Turkson, J., Ryan, D., Kim, J. S., Zhang, Y., Chen, Z., Haura, E., Laudano, A., Sebti, S., Hamilton, A. D., and Jove, R. (2001). Phosphotyrosyl peptides block Stat3-mediated DNA binding activity, gene regulation, and cell transformation
14. *J.Biol.Chem.* **276**, 45443-45455.

Udy, G. B., Towers, R. P., Snell, R. G., Wilkins, R. J., Park, S. H., Ram, P. A., Waxman, D. J., and Davey, H. W. (1997). Requirement of STAT5b for sexual dimorphism of body growth rates and liver gene expression. *Proc.Natl.Acad.Sci.U.S.A* **94**, 7239-7244.

van Puijenbroek, A. A., van der Saag, P. T., and Coffer, P. J. (1999). Cytokine signal transduction in P19 embryonal carcinoma cells: regulation of Stat3-mediated transactivation occurs independently of p21ras-Erk signaling. *Exp.Cell Res.* **251**, 465-476.

Wang, B., Soule, H. D., and Miller, F. R. (1997). Transforming and oncogenic potential of activated c-Ha-ras in three immortalized human breast epithelial cell lines. *Anticancer Res.* **17**, 4387-4394.

Wang, T., Niu, G., Kortylewski, M., Burdelya, L., Shain, K., Zhang, S., Bhattacharya, R., Gabrilovich, D., Heller, R., Coppola, D., Dalton, W., Jove, R., Pardoll, D., and Yu, H. (2004). Regulation of the innate and adaptive immune responses by Stat-3 signaling in tumor cells. *Nat.Med.* **10**, 48-54.

Williams, L. T., Escobedo, J. A., Fantl, W. J., Turck, C. W., and Klippel, A. (1991). Interactions of growth factor receptors with cytoplasmic signaling molecules. *Cold Spring Harb.Symp.Quant.Biol.* **56**, 243-250.

Xia, Z., Baer, M. R., Block, A. W., Baumann, H., and Wetzler, M. (1998). Expression of signal transducers and activators of transcription proteins in acute myeloid leukemia blasts. *Cancer Res.* **58**, 3173-3180.

Xu, X., Sun, Y. L., and Hoey, T. (1996). Cooperative DNA binding and sequence-selective recognition conferred by the STAT amino-terminal domain. *Science* **273**, 794-797.

Yoshikawa, H., Matsubara, K., Qian, G. S., Jackson, P., Groopman, J. D., Manning, J. E., Harris, C. C., and Herman, J. G. (2001). SOCS-1, a negative regulator of the JAK/STAT pathway, is silenced by methylation in human hepatocellular carcinoma and shows growth-suppression activity. *Nat.Genet.* **28**, 29-35.

Zamo, A., Chiarle, R., Piva, R., Howes, J., Fan, Y., Chilosi, M., Levy, D. E., and Inghirami, G. (2002). Anaplastic lymphoma kinase (ALK) activates Stat3 and protects hematopoietic cells from cell death. *Oncogene* **21**, 1038-1047.

Zhang, Q., Raghunath, P. N., Xue, L., Majewski, M., Carpentieri, D. F., Odum, N., Morris, S., Skorski, T., and Wasik, M. A. (2002a). Multilevel dysregulation of STAT3 activation in anaplastic lymphoma kinase-positive T/null-cell lymphoma. *J.Immunol.* **168**, 466-474.

Zhang, Y., Turkson, J., Carter-Su, C., Smithgall, T., Levitzki, A., Kraker, A., Krolewski, J. J., Medveczky, P., and Jove, R. (2000). Activation of Stat3 in v-Src-transformed fibroblasts requires cooperation of JAK1 kinase activity. *J.Biol.Chem.* **275**, 24935-24944.

Zhang, Y. W., Wang, L. M., Jove, R., and Vande Woude, G. F. (2002b). Requirement of Stat3 signaling for HGF/SF-Met mediated tumorigenesis. *Oncogene* **21**, 217-226.

Zvelebil, M. J., Panayotou, G., Linacre, J., and Waterfield, M. D. (1995). Prediction and analysis of SH2 domain-phosphopeptide interactions. *Protein Eng* **8**, 527-533.

CURRICULUM VITAE

EDUCATION

1983-1995:	German School in Barcelona ("Allgemeine Deutsche Hochsculreife"/"Bachillerato")
1995-2000:	Pharmacy studies at the University of Barcelona ("Licenciatura" i.e. equivalent to a "Staatsexamen")
2000-2002:	Master in Science in Molecular Oncology and Immunology at New York University
2002-2004:	PhD at Merck Darmstadt

SCIENTIFIC TRAINING

1998:	University of Pharmacy (Barcelona) Training at the biochemistry department
summer 1998:	Wyeth Pharma (Münster) Training at the quality control department
1998-1999:	Merck Bioresearch laboratory (Barcelona) Training at the oncology research department
summers 1999 and 2000:	Abbott (Ludwigshafen) Training at the development department for parental solutions
1999-2000:	University of Pharmacy (Barcelona) Training at the biopharmacy department
2000-2002:	New York Univerisity (New York) Master in Science in Molecular Oncology and Immunology

EIDESTATTLICHE ERKLÄRUNG

Hiermit erkläre ich des Eides statt, dass ich die vorliegende Dissertation nur mit den angegebenen Hilfsmitteln angefertigt habe. Ich habe noch keinen Promotionsversuch unternommen.

Ana Aubert-Jürgens